EPA-460/3-74-001

DIESEL FUEL INJECTION SYSTEM SIMULATION AND EXPERIMENTAL CORRELATION

U.S. ENVIRONMENTAL PROTECTION AGENCY
Office of Air and Water Programs
Office of Mobile Source Air Pollution Control
Emission Control Technology Division
Ann Arbor, Michigan 48105

EPA-460/3-74-001

DIESEL FUEL INJECTION SYSTEM SIMULATION AND EXPERIMENTAL CORRELATION

Prepared by

J. A. Bolt, M. F. El-Erian, and E. B. Wylie

Automotive Engineering Laboratory
Department of Mechanical Engineering
College of Engineering
The University of Michigan
Ann Arbor, Michigan 48105

Grant No. R800 424

EPA Project Officer:

Dr. Jose L. Bascunana

Prepared for

U.S. ENVIRONMENTAL PROTECTION AGENCY
Office of Air and Water Programs
Office of Mobile Source Air Pollution Control
Emission Control Technology Division
Ann Arbor, Michigan 48105

Januany 1974

This report is issued by the Environmental Protection Agency to report technical data of interest to a limited number of readers. Copies are available free of charge to Federal employees, current contractors and grantees, and nonprofit organizations - as supplies permit - from the Air Pollution Technical Information Center, Environmental Protection Agency, Research Triangle Park, North Carolina 27711, or from the National Technical Information Service, 5285 Port Royal Road, Springfield, Virginia 22151.

This report was furnished to the Environmental Protection Agency by the Automotive Engineering Laboratory, Ann Arbor, Michigan, in fulfillment of Grant No. R800 424. The contents of this report are reproduced herein as received from the Automotive Engineering Laboratory. The opinions, findings, and conclusions expressed are those of the author and not necessarily those of the Environmental Protection Agency. Mention of company or product names is not to be considered as an endorsement by the Environmental Protection Agency.

Publication No. EPA-460/3-74-001

ABSTRACT

After-injection is the term used to describe the introduction of additional fuel into the combustion chamber of a diesel engine after the end of the normal injection. After-injection is caused by uncontrolled pressure transients in the injection system after the opening of the pump spill port. These pressure transients are related to the wave propagation phenomena in the high-pressure pipeline connecting the pump and injector. It is a persistent diesel fuel injection system problem which results in reduced engine power and economy and increased emissions.

A theoretical digital simulation of a conventional diesel fuel injection system was developed. The influence of such factors as wave progagation phenomena, pipe friction, and cavitation are included. The computer results are compared with transient pressures as measured on an actual fuel injection system operated on a test bench. The comparisons show the accuracy and validity of this simulation method. Special attention is given to some of the important factors that affect the accuracy of the simulation model. These include the effect of pressure on the fuel bulk modulus and wave speed, the pipeline residual pressure, and the coefficient of discharge of important orifices.

Analytical control methods were developed to help determine design means by which after-injection may be controlled. Further investigation and evaluation of two design changes which release the injection system excess elastic energy in a controlled manner are considered in the report. One design change consists of the addition of a control valve in the pump delivery chamber. The other involves the modification of the pump spill port. In both cases, pressures and flows are not significantly altered during the main injection period. The ability of both design changes to control after-injection is confirmed by the use of a simulation program. Experimental data from a system with the pump spill port modified in accordance with theoretical design calculations provided satisfactory confirmation of the analyses.

SUMMARY

Difficult problems exist in diesel fuel injection systems due to pressure waves and other highly transient phenomena in the high pressure lines and other components. Among other problems, these transient pressure phenomena commonly give rise to a condition known as after-injection, the name used to denote a condition when the fuel spray nozzle discharges an additional quantity of fuel after the normal fuel delivery. After-injection is mainly the result of pressure wave phenomena traveling the length of the line connecting the pump and nozzle. It can also result from other sources of elasticity in the complete system.

We believed, based on experience, and from talking to many engineers very familiar with diesel engines, that this condition of after-injection was much more prevalent and a greater handicap to good engine performance than has been indicated by the technical literature concerning diesel engines. In recent years there has been conjecture concerning the effect of after-injection on diesel engine exhaust emissions and smoke.

Interest in this project concerning diesel fuel injection system simulation also arose in part from our research work done for the U.S. Army Tank Automotive Command (TACOM). This work for the Army under contracts* during the past eight years was concerned with ignition delay and combustion phenomena under conditions of high supercharging pressure, and with high cylinder coolant temperatures. In the course of this work we first used a single-cylinder Lister-Blackstone diesel engine, and later the U.S. Army Tank Command (TACOM) engine built by the International Harvester Company. The TACOM engine had substantial amounts of after-injection at many operating conditions which seriously affect the reproducibility of data, the engine performance, and exhaust emissions. These technical difficulties are described in a final Army report listed below.**

A much more complete understanding of the transient phenomena in the jerk-pump injection system (for example, as made by American Bosch) was gained by developing a digital computer simulation program. The results of this program were checked experimentally by means of a one-cylinder fuel injection system tested on a bench test rig. This system was the same as that used on the TACOM research engine.

---

*Contract Numbers DAAE07-71-C-0248 and DAAE07-69-1289.

**U.S. Army Tank Automotive Command, Technical Report No. 11796, entitled, "Diesel Engine Combustion and Emissions—TACOM Research Engine," by Bolt, El-Erian, Duerr, and Milkos, April, 1973.

The analytical studies and digital simulation work was greatly aided by enlisting the help of Professors E. Benjamin Wylie and Victor L. Streeter of The University of Michigan, Department of Civil Engineering, who are well known for their simulation of transient phenomena in large hydraulic power systems. They, with our graduate students, applied the method of characteristics to the relatively small diesel systems. As a result of this work, one doctoral thesis was prepared, and three SAE papers were published. These describe in detail the technical work done and the results accomplished. These are as follows:

1. "Diesel Fuel Injection System Simulation and Experimental Correlation, by E. Benjamin Wylie, Jay A. Bolt, and Mohamed F. El-Erian, Society of Automotive Engineers, Paper No. 710569, June, 1971, SAE Trans., Vol. 80, 1971.

2. "Simulation and Control of Transient Flow in the Diesel Injection System," Mohamed F. El-Erian. A University of Michigan doctoral thesis, published in 1972.

3. "Analysis and Control of Transient Flow in the Diesel Injection System, Part I - The Analytical Control Method," by Mohamed F. El-Erian, E. Benjamin Wylie, and Jay A. Bolt, Society of Automotive Engineers, Paper No. 730661, June, 1973, SAE Trans., Vol. 82, 1973.

4. "Analysis and Control of Transient Flow in the Diesel Injection System, Part II - Design Results of Controlled After-Injection," by Mohamed F. El-Erian, E. Benjamin Wylie, and Jay A. Bolt, Society of Automotive Engineers, Paper No. 730662, June, 1973, SAE Trans., Vol. 82, 1973.

The body of this report consists of the three papers listed above, which are attached at the end of this report. The doctoral thesis of M. F. El-Erian, item 2 above, also contains much detailed information concerning the simulation work. Copies of this University of Michigan thesis, consisting of 151 pages, are available from University Microfilms, 300 N. Zeeb Road, Ann Arbor, Michigan, for approximately $15.00

Under the grant we had hoped to install the standard and modified injection systems on the TACOM research diesel engine. This would make it possible to operate the injection system and engine with or without after-injection, with all other conditions being held constant. This would permit us to obtain accurate quantitative data on the effect of after-injection on diesel engine performance, emissions, and smoke. However, unforeseen difficulties with the test equipment made it impractical to complete this phase of the project before the grant funds were exhausted.

We are, however, now doing this comparative testing with very limited research funds available from several small industry research grants provided to the Department of Mechanical Engineering for graduate student support.

With this support a doctoral student from Nigeria, Mr. Sam Onyegegbu, is proceeding with this comparative testing as the topic of his doctoral thesis.

We are hopeful that will will obtain reliable data suitable for publication showing the effect of known amounts and characteristics of after-injection on the performance, emissions, and smoke from diesel engines.

ACKNOWLEDGMENT

This investigation was supported by the United States Environmental Protection Agency, as indicated on the cover sheet. The cooperation of the following persons is greatly appreciated: Dr. Jose Bascunana of the EPA; Mr. Floyd Lux, George Cheklich, and others of the U.S. Army Tank-Automotive Command. The valuable contributions of doctoral students Bela Petry and Sam Onyegegbu are also appreciated.

SOCIETY OF AUTOMOTIVE ENGINEERS, INC.
Two Pennsylvania Plaza, New York, N.Y. 10001

Diesel Fuel Injection System Simulation and Experimental Correlation

E. Benjamin Wylie, Jay A. Bolt, and Mohamed F. El-Erian
University of Michigan

SOCIETY OF AUTOMOTIVE ENGINEERS

Mid-Year Meeting
Montreal, Que., Can.
June 7-11, 1971

710569

710569

Diesel Fuel Injection System Simulation and Experimental Correlation

E. Benjamin Wylie, Jay A. Bolt, and Mohamed F. El-Erian
University of Michigan

THE PURPOSE OF THIS PAPER is to report transient phenomena measured in a diesel fuel injection system and to describe an analytical simulation of the system. Comparisons are made between experimental and computed data for several different operating conditions of the injection system. The characteristics unique to this simulation are discussed in some detail.

A diesel fuel injection system is an assembly of many complex and intricate mechanical components, each with a specific function. In addition to the behavior of individual components, the interaction of these components has an important influence on the ultimate operation of the system. The response of the fuel injector is primarily dependent upon the action of the pump and the pressure wave propagation phenomena in the delivery pipeline. The pump action, with its delivery chamber and valve, is not independent of the injector and delivery pipeline; that is, a complete system interaction takes place.

An understanding of the detailed operation of individual components in the system and the influence of design parameters on this operation are the desired objectives. With such information available in an analytical simulation, perhaps design changes may be identified to improve nozzle fuel spray characteristics, to eliminate the secondary after-injection, and to generally improve the engine combustion characteristics with a view towards reduced smoke and exhaust emissions.

In this paper, following a brief review of the topical literature, the analytical model and experimental apparatus are described. Comparisons between simulated and experimental results are then presented, followed by a critical review of the results. Significant parameters and control variables are identified and discussed, and the usefulness of the analytical simulation is intimated.

LITERATURE REVIEW

A great variety of procedures have been used to study the diesel injection system, some experimental and others theoretical in nature. Before 1960, the injection simulation studies were limited due to the requirement of lengthy mathematical computations. This disadvantage made it impractical to apply theoretical simulation in the design stage and led to experimental trial-and-error procedures. Analytical studies were completed only after the introduction of many simplifying assumptions.

ABSTRACT

A theoretical digital simulation of a conventional diesel fuel injection system has been developed. The influence of such factors as wave propagation phenomena, pipe friction, and cavitation are included. The computer results are compared with transient pressures as measured on an actual fuel injection system operated on a test bench. The comparisons show the accuracy and validity of this simulation scheme. Special attention is given to some of the important factors that affect the accuracy of the simulation model. These include the effect of pressure on the fuel bulk modulus and wave speed, the pipe line residual pressure, and the coefficient of discharge of important orifices.

One of the earliest significant contributions relative to fuel injection systems is due to Davis and Giffen (1)*. Their discussion includes mention of many of the significant variables involved in the system: fluid compressibility, elastic deformation, pressure wave propagation, fluid friction, and pump and nozzle characteristics, including secondary injection.

De Juhasz (2), used graphical water hammer concepts to provide an analysis of a linear model of typical simplified injection systems, including the elements of the pipeline, pump, nozzle, and a fluid volume.

Giffen and Row (3), theoretically solved the equations representing the injection system, taking into account the effect of pressure waves in the delivery pipe and the capacity effects of the volumes concentrated in the pump and nozzle system. They handled the differential equations by placing them in finite difference form and finding an algebraic expression for the solution. This method of solution was limited to simple injection models because of the time required for mathematical solutions.

Knight (4), introduced a model for viscous friction and cavitation in the delivery pipe, and used the same model for the pump and nozzle system described in Ref. 3. His calculations were performed on a digital computer.

Becchi (5), used a model which comprised a detailed representation of the injector and the pump, but he neglected friction in the delivery pipe and had no provision for possible occurrence of vapor cavities. He solved the system of differential equations by an iterative method after writing them in finite difference form.

Brown and McCallion (6), combined Becchi's detailed representation of the pump and injector with a model that included viscous friction and possible cavitation in the delivery pipe. They also considered a detailed modeling of the delivery valve as described by Stone (7), and solved the system of equations by another iterative method.

The work of Walwijk, Van der Graaf, and Jansen (8) is also to be noted. Their experimental apparatus enabled them actually to measure the motion of the delivery valve and injector needle, as well as the pressure in various locations in the system. Particular attention was devoted to the motion of the delivery valve in their simulation on a digital computer. A good correlation was achieved between experimental and computed results.

All of the investigators discuss some of the factors that are likely to affect the accuracy of the model. The value of the delivery pipeline base pressure is important for a meaningful comparison between the model and experimental results. A treatment of vapor pressure in the delivery pipeline is also needed for a complete model. Kreith and Eisentadt (9), and Lichtarowicz, Duggins, and Markland (10), presented experimental results of the variation of the coefficient of discharge over a wide range of Reynolds number and length-to-diameter ratio. Giffen and Row (3) cautioned of the danger of using coefficients of discharge from the literature. They preferred to use experimentally determined values for the particular nozzle under consideration. The data of Gelalles (11), in which he tested different nozzle configurations, showed that the coefficient of discharge, besides depending on length-over-diameter ratio and Reynold's number, is also greatly dependent on the configuration of the reservoir leading to the nozzle holes.

Recent investigators also give considerable attention to the stability and convergence of their solutions. Henrici (12), discusses three different methods of numerical solution of a system of differential equations: the iterative solution of simultaneous algebraic equations, the expansion methods (Taylor's method or Runge Kutta method), and the numerical integration methods. The third method includes the predictor-corrector method which offers the advantage of an adjustable time increment, dependent upon a given error bound. This particular advantage is of great value especially for reducing computation time. The first and second methods require the use of very small time steps and a prior knowledge of the size of the time step.

ANALYTICAL MODEL

A schematic representation of the system is shown in Fig. 1 and includes three major components: the fuel pump, the connecting fuel line, and the fuel injector. The analytical model, which is programmed for a time variant simulation on the digital computer, must include an accurate description of the geometric and physical character of the system, as well as the equations that describe the dynamics of the fluid and mechanical components. A total system analysis is necessary wherein the ordinary differential equations which describe fluid compressibility, delivery valve motion, and injector needle motion, are handled numerically simultaneously with the numerical solution of the partial differential equations that describe the wave propagation phenomena in the fuel lines.

Prior to the description of the formulation of equations and the method of solution, the underlying assumptions in this simulation are set forth. Fluid compressibility is introduced by use of the bulk modulus of elasticity. The variation of bulk modulus, and the variation of fluid density, with pressure is also considered (13, 14). All elastic deformations of solid parts of the system due to pressure changes are neglected. The foregoing assumptions yield a pressure-dependent wave propagation velocity that is a function of fluid compressibility only. The error in wave velocity as a result of neglecting pipeline deformation is less than 0.5% for the maximum pressure variation. A distributed parameter one-dimensional model is used to describe flow in the fuel lines. This implies that the parameters of compliance, inertia, and frictional losses are distributed along the pipeline. Frictional effects are evaluated by considering the loss during unsteady flow to be the same as the loss for steady flow at the same velocity and fluid property. A friction-factor-resistance formulation is used wherein the factor is a function of Reynolds number. If vapor pressure is reached at any point in the system, a vapor cavity is permitted to grow and collapse in accordance with the dynamic equations and a local mass continuity balance. Orifice discharge

*Numbers in parentheses designate References at end of paper.

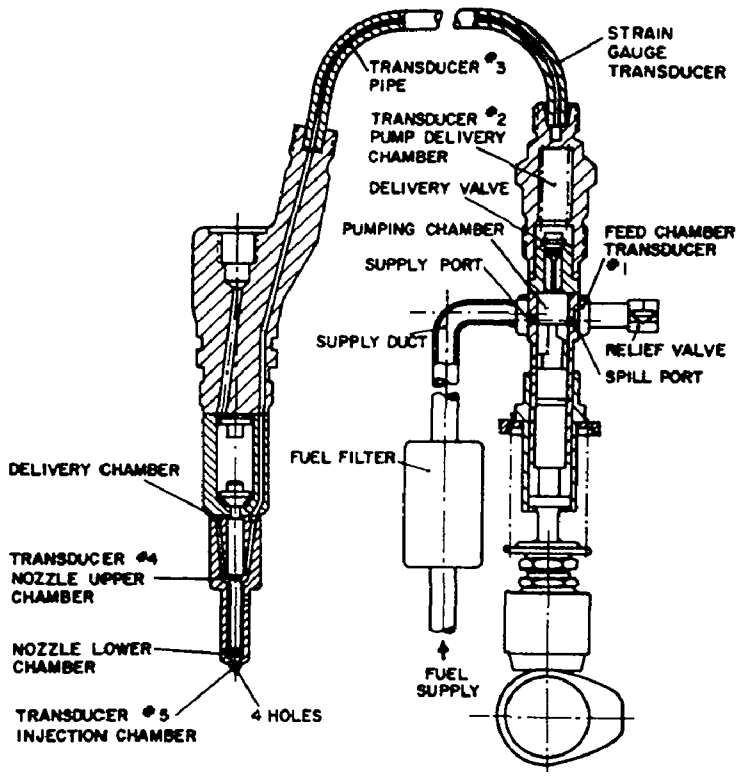

Fig. 1 - Schematic representation of diesel injection system and points of pressure measurement

coefficients are based upon steady-state data and may be Reynolds number dependent.

THEORETICAL FORMULATION OF MODEL - The equations to describe the dynamic response of the system are grouped into three categories: the pipeline, the pump, and the injector.

Transient behavior of a compressible fluid in a pipeline may be described by the general equations of motion and continuity applied to an elemental length of the pipe. The equation of motion is expressed in the following form (15):

$$\frac{\partial Q}{\partial t} + \frac{gA}{\gamma}\frac{\partial p}{\partial x} + \frac{f}{2DA} Q|Q| = 0 \qquad (1)$$

where:

- p = Pressure
- Q = Volumetric flow rate
- A = Pipe cross-sectional area
- g = Acceleration of gravity
- D = Pipe diameter
- f = Darcy-Weisbach friction factor
- γ = Unit weight of fluid
- x and t = Independent variables distance and time.

The absolute value sign is used on the friction term so the equation is valid for negative flow. The continuity equation for a horizontal pipeline is:

$$\frac{\partial Q}{\partial x} + \frac{gA}{a^2\gamma}\frac{\partial p}{\partial t} = 0 \qquad (2)$$

where:

- a = Wave propagation velocity in fluid, defined by $a = \sqrt{gK/\gamma}$,
- K = Bulk modulus of elasticity.

The convective acceleration terms in Eqs. 1 and 2 have been dropped as, in general, they are of much smaller order than the terms shown.

Eqs. 1 and 2 are transformed, by use of the method of characteristics (15) into two ordinary differential equations, each of which is valid along a particular characteristic line. When these equations are placed in finite-difference form by a first-order approximation of the integration, they become:

$$Q_Z - Q_W + \frac{gA}{\gamma_W a_W}(p_Z - p_W) + \frac{f_W \Delta t Q_W |Q_W|}{2DA} = 0 \qquad (3)$$

$$x_Z - x_W = a_W \Delta t \qquad (4)$$

$$Q_Z - Q_Y - \frac{gA}{\gamma_Y a_Y}(p_Z - p_Y) + \frac{f_Y \Delta t Q_Y |Q_Y|}{2DA} = 0 \qquad (5)$$

$$x_Z - x_Y = - a_Y \Delta t \qquad (6)$$

where:

subscripts = Positions in x-t plane as shown in Fig. 2.

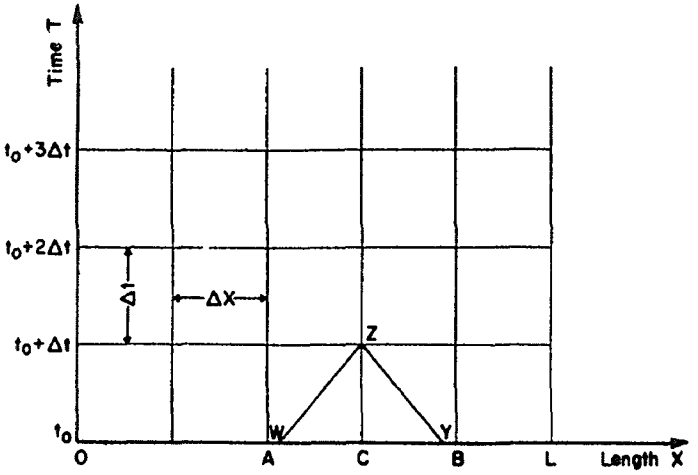

Fig. 2 - Characteristics in x-t plane

Eq. 3 is valid only along the forward characteristic line, W-Z, described by Eq. 4, and Eq. 5 is valid only along a receding characteristic line, Y-Z, described by Eq. 6. An analysis of any pipeline begins with known conditions at time, $t = t_0$; then calculations of transient pressures and discharges are made at fixed, equally spaced sections throughout the pipe. For stability reasons it is necessary that the grid spacing, Δx, must be greater than or equal to the product of the wave speed a, and Δt. In Fig. 2, assume p and Q are known at each grid intersection along the axis $t = t_0$. At point Z, new values of p and Q may be calculated by use of Eqs. 3 and 5. In order to accomplish this solution, it is necessary to interpolate between known conditions at A and C to find the values at W. This interpolation is necessary since the variable wave speed may position W at any location between A and C. A similar interpolation is necessary at Y. All interior grid intersection points at $t_0 + \Delta t$ are computed in the manner described above. At $x = 0$, the receding characteristic Eq. 5 is solved simultaneously with the boundary condition equations. At $x = L$, the forward characteristic Eq. 3 is solved with the downstream boundary condition. When new values of flow and pressure have been computed at each grid point at $t = t_0 + \Delta t$, time is incremented to $t_0 + 2\Delta t$, and the solution is obtained at the next higher set of grid points. The pipe end conditions to be used in this problem include the injector needle at the downstream end of the fuel delivery line, the pump at the upstream end of the fuel delivery line and also at the downstream end of the fuel supply duct, and a constant pressure supply at the upstream end of the fuel supply duct.

The equations to describe the dynamic action of the pump and fuel injector must include:

1. A description of the compressibility of fluid in the various volumes, of the following form:

$$K = \frac{\Delta p}{\Delta \forall / \forall} \tag{7}$$

where:

K = Bulk modulus of fluid
$\forall$ = Volume of enclosure

2. An unsteady continuity equation written for each volume: the net mass inflow into an enclosure at an instant must be equal to the time rate of increase of mass within the enclosure.

3. An equation of motion to describe the forces and dynamic action of mechanical parts such as the delivery valve:

$$\Sigma F = m\, dV/dt \tag{8}$$

where:

ΣF = Sum of all pressure, frictional, and spring forces in the direction of motion
m = Mass of object
V = Velocity

4. An equation to describe the flow rate through the various ports and orifices, of the form:

$$Q = C_d A \sqrt{\frac{2g}{\gamma}(p_1 - p_2)} \tag{9}$$

where:

C_d = Discharge coefficient
A = Instantaneous area of opening
$(p_1 - p_2)$ = Pressure drop across opening

Pump equations, for the elements shown in Fig. 3, are as follows. Eq. 7 and the continuity equation for each of the feed chamber, pump chamber, and delivery chamber are, respectively:

$$\frac{d\, p_f}{dt} = \frac{K_f}{\forall_f}(Q_{Zs} - Q_1 + Q_2 - Q_4) \tag{10}$$

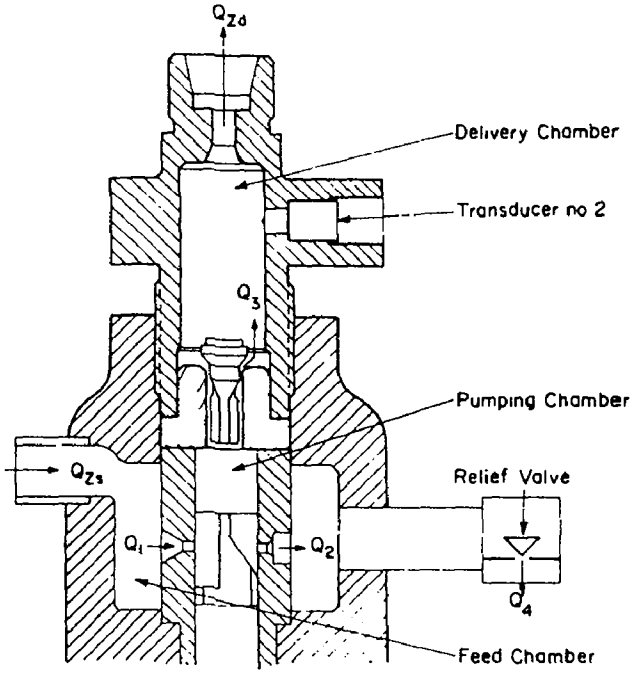

Fig. 3 - Sectional view of injection pump

$$\frac{d\,p_p}{dt} = \frac{K_p}{\forall_p + A_v S_v - A_p S_p}(A_p V_p - A_v V_v + Q_1 - Q_2 - Q_3) \tag{11}$$

$$\frac{d\,p_d}{dt} = \frac{K_d}{\forall_d - A_v S_v}(A_v V_v + Q_3 - Q_{Zd}) \tag{12}$$

Eq. 8 applied to the delivery valve becomes

$$\frac{d\,V_v}{dt} = \frac{g}{W_v}(A_v(p_p - p_d) - k_v - r_v S_v - f_v V_v) \tag{13}$$

and

$$\frac{d\,S_v}{dt} = V_v \tag{14}$$

In these equations the subscripts f, p, d, and v refer to the feed chamber, pumping chamber, pump delivery chamber, and delivery valve, while flows with numerical subscripts refer to orifice flows, Fig. 3, and are defined by Eq. 9:

$$Q_1 = C_{d_1} A_1 \sqrt{2g(p_f - p_p)/\gamma} \tag{15}$$

$$Q_2 = C_{d_2} A_2 \sqrt{2g(p_p - p_f)/\gamma} \tag{16}$$

$$Q_3 = C_{d_3} A_3 \sqrt{2g(p_p - p_d)/\gamma} \tag{17}$$

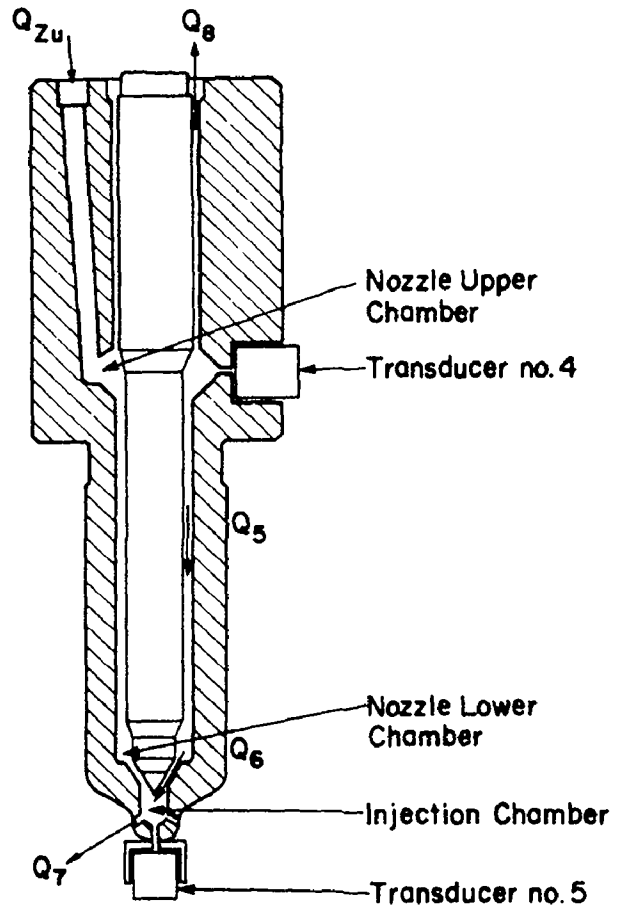

Fig. 4 - Sectional view of injection nozzle

$$Q_4 = C_{d_4} A_4 \sqrt{2g\,p_f/\gamma} \tag{18}$$

The flow Q_{ZS} is in the supply duct, defined by Eq. 3, and Q_{Zd} is in the delivery pipe and is defined by Eq. 5. The quantities S, k, r, f, and W refer to valve displacement, spring force, spring stiffness, friction coefficient, and valve weight, respectively.

Fuel injector equations, Fig. 4, take a similar form. The delivery and nozzle upper chambers, nozzle lower chamber, and injection chamber relations are:

$$\frac{d\,p_u}{dt} = \frac{K_u}{\forall_u + A_u S_n}(Q_{Zu} - Q_5 - Q_8 - A_u V_n) \tag{19}$$

$$\frac{d\,p_l}{dt} = \frac{K_l}{\forall_l + A_l S_n}(Q_5 - Q_6 - A_l V_n) \tag{20}$$

$$\frac{d\,p_i}{dt} = \frac{K_i}{\forall_i + A_i S_n}(Q_6 - Q_7 - A_i V_n) \tag{21}$$

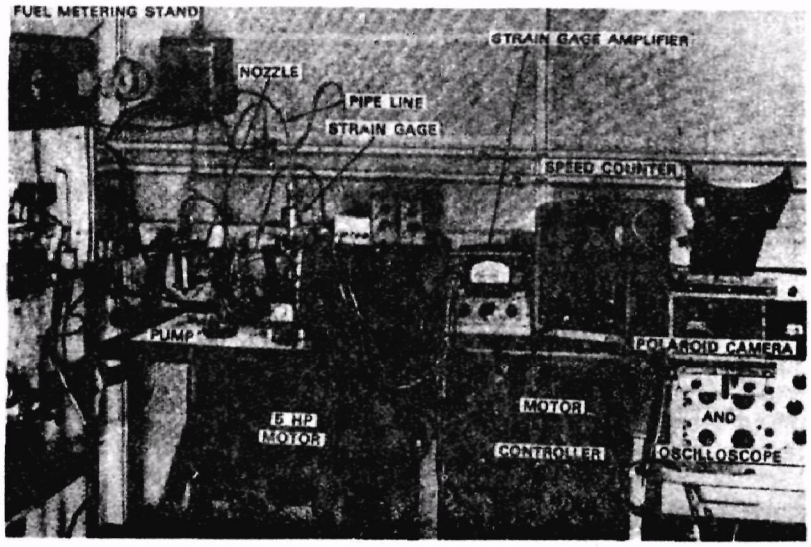

Fig. 5 - Diesel fuel injection system test equipment

Eq. 8 applied to the needle becomes

$$\frac{d\,V_n}{dt} = \frac{g}{W_n}(A_u p_u + A_l p_l + A_i p_i - k_n - r_n S_n - f_n V_n) \tag{22}$$

and

$$\frac{d\,S_n}{dt} = V_n \tag{23}$$

The subscripts u, l, i, and n refer to the upper nozzle and delivery chambers, the lower nozzle chamber, the injector chamber, and the injector needle. The flow Q_{Zu} refers to the end of the delivery pipe and is given by Eq. 3. The orifice flows, Fig. 4, are:

$$Q_5 = C_{d_s} A_5 \sqrt{2g\,(p_u - p_l)/\gamma} \tag{24}$$

$$Q_6 = C_{d_6} A_6 \sqrt{2g\,(p_l - p_i)/\gamma} \tag{25}$$

$$Q_7 = C_{d_7} A_7 \sqrt{2g\,(p_i - p_c)/\gamma} \tag{26}$$

and leakage by the needle given by

$$Q_8 = C_8\, p_u \tag{27}$$

In Eq. 26, p_c is the pressure in the combustion chamber, and in Eq. 27, C_8 is a viscous flow coefficient and function of the area of flow and fluid properties.

METHOD OF SOLUTION - The procedure for numerical solution of the partial differential Eqs. 1 and 2 by the method of characteristics is well documented in the literature (15), and results from such computations have been verified experimentally. To obtain an accurate simulation of the complete system, the pump and injector are treated as boundary conditions for the pipeline and are solved at the identical time step as the pipeline. Due to the extremely rapid response time of the boundaries, particular care must be exercised to be assured of a true solution to each set of ordinary differential equations (Eqs. 10-14 and 19-23). Neither an iterative nor Runge-Kutta approximation could be successfully applied at time steps that were economically feasible for the method of characteristics. A modified predictor-corrector method by Hamming (16) is used in this model. This procedure offers the advantage of being able to reduce the step size within a fixed characteristics method time step in order to achieve a desired accuracy level. Thus, during portions of the cycle, when the transient contains high frequency components, a relatively small step size is used, whereas a step size equal to the characteristics time step is adequate over the major part of the cycle. The predictor-corrector method makes use of the system response at earlier times; additionally it requires information from the pipeline during the step change. The latter information is available from the characteristics described in Eqs. 3-6.

With the characteristics method solution in the pipelines and the characteristics interfacing with the predictor-corrector solution of the boundary equations, a solution for the total system response is possible. The forcing function for the entire system is the specified cam motion which drives the pump plunger.

During the transient response, if the pressure tends to drop below vapor pressure at any point in the system, the pressure at the point is set equal to vapor pressure, and a vapor cavity is assumed to form instantaneously. A local mass continuity condition is established to simulate the growth and decay of the vapor cavity. When the cavity collapses, the solution procedure returns to normal computations.

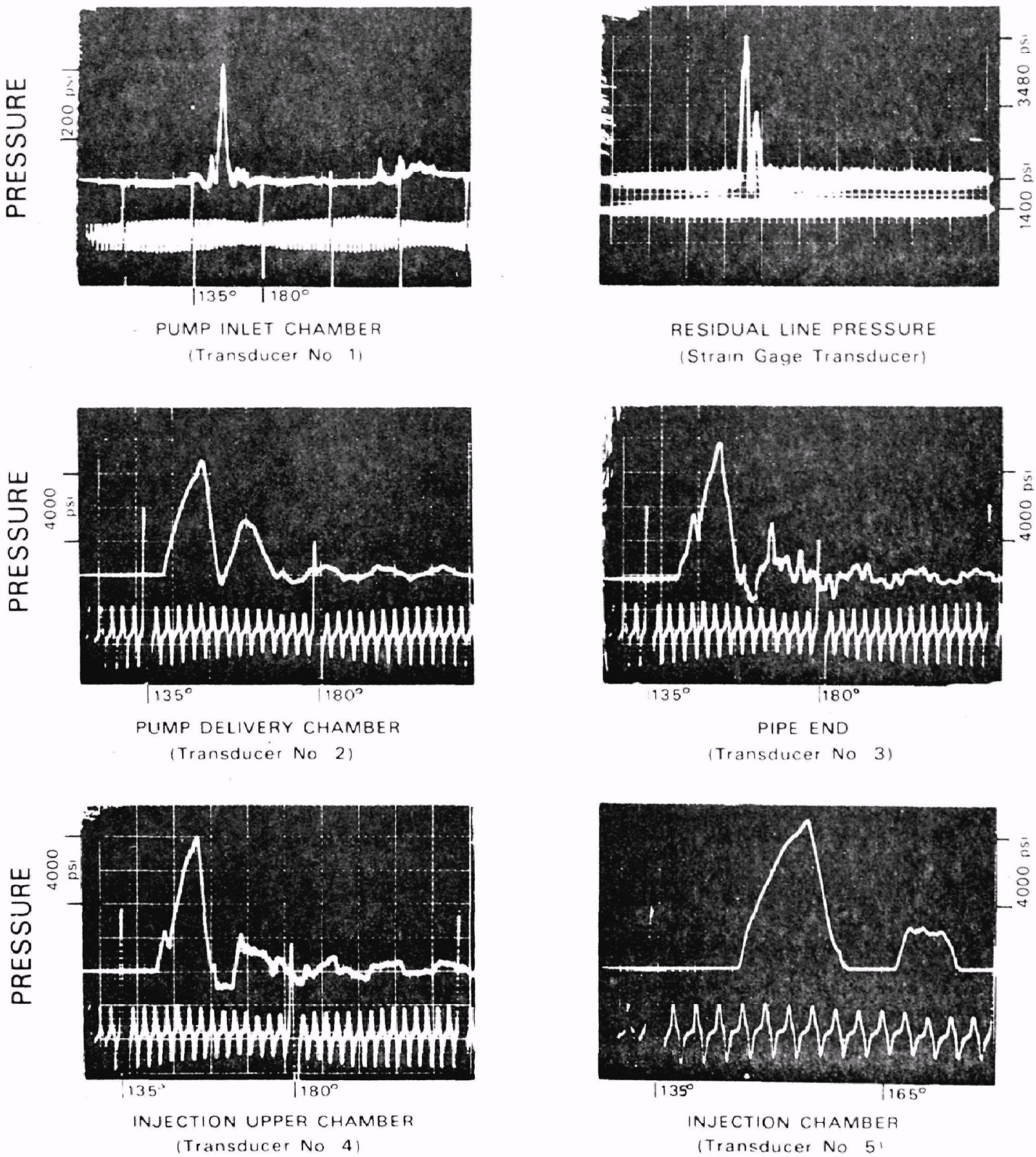

Fig. 6 - Oscilloscope records of transient phenomena in injection system

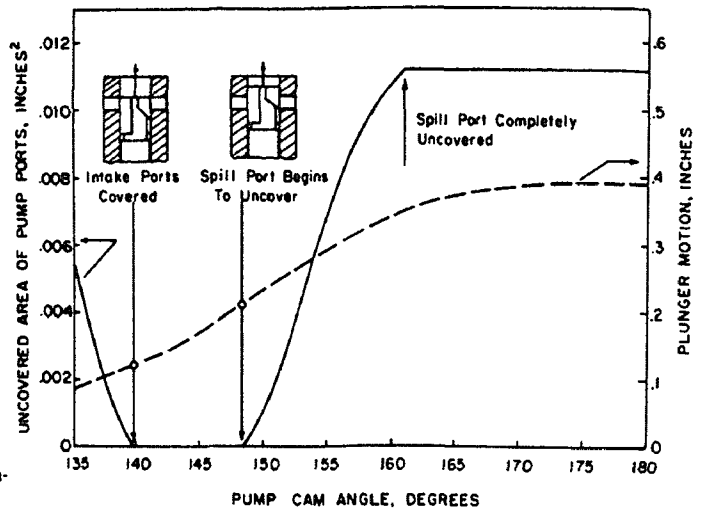

Fig. 7 - Pump plunger motion and pump port areas; rack control setting = 0.509 in.

EXPERIMENTAL EQUIPMENT, INSTRUMENTATION, AND RESULTS

The experimental apparatus and test results are described, followed by a comparison of computed and experimental results. The purpose of the equipment is to determine quantitatively the time variant response of the predominant variables in the apparatus during a normal operating cycle. Practically, it is impossible to measure all variables, nor is it necessary. One of the primary objectives is to provide enough information to confirm the analytical simulation of the operating system. As already discussed, the analytical model must treat each component part in great detail. A satisfactory confirmation is acknowledged if the simulation provides agreement with the experiment in a random sample of the dependent variables. To accomplish this objective in a given test, the system geometric configuration and fluid properties must be identified, and the pump speed and volumetric fuel supply setting must be known. The system response is then identified by transient pressure measurements at specific locations; a measurement of fuel input at the pump and a measurement of fuel injected at the nozzle. The latter measurements are averaged over a number of cycles with the difference between the two quantities representing the system leakage.

A general view of the diesel injection test bench is shown in Fig. 5. This shows the injection pump mounted on a stand. The pump is an American Bosch APEIB type and has a plunger diameter of 10 mm. The pump is connected to the injector by a high pressure pipe line 0.067 in. inside diameter, 0.25 in. outside diameter, and 36.4 in. long. The injector is an American Bosch ADB-150S type, and has a 4-hole nozzle of 0.012 in. diameter each. The pump drive system includes a substantial flywheel to provide uniform rotation and is driven by a variable speed d-c motor. The speed is variable within the range, 100 rpm-1000 rpm. The fuel rack is positioned by a micrometer that has a travel between 0 and 1 in., corresponding to maximum fuel and minimum fuel delivery, respectively, with a minimum graduation of 0.001 in. Refs. 17 and 18 were very helpful in the design and construction of the test equipment.

The net fuel flow to the pump is measured using a metering stand (left side of Fig. 5) which consists of a balance, a relay system and an electric clock. The injected fuel is collected and weighed. The fuel pressure is measured using AVL piezo quartz pressure transducers. Fig. 1 shows the location of the five pressure transducers. Further details of the transducer location connections are shown in Figs. 3 and 4. An additional strain gage-type static pressure transducer is positioned on the pipeline directly above the pump. This unit was constructed and added to the pipeline to measure the fuel line residual pressure during tests. A Tektronics 502A type dual beam oscilloscope with a polaroid camera was used to record the pressure traces.

The cam angles were measured every 3 deg, using a disc with 120 equally spaced holes mounted on the flywheel and an electro-magnetic pick up, type 3010-AN, (made by Electro-Mation Co.). The injector opening pressure for all tests was set at 3000 lb/in.^{2}, under quasi-static conditions. The fuel used in these tests was Standard Oil Co. No. 2 diesel fuel.

A sample of the recorded pressure traces are displayed in Fig. 6, representing a pump speed of 800 rpm, rack micrometer setting of 0.509 which corresponds to a fuel injection rate of 0.19 lb/min, and system base pressure (residual line pressure) of 1400 psi. The upper line in each frame is the pressure trace taken at each transducer location shown in Fig. 1. The lower trace correlates the pressure trace with the instantaneous position in the pumping cycle. The plunger motion and the area of the spill port are shown for this case in Fig. 7.

The experimental data obtained with this equipment are very reproducible. That is, if identical test conditions are set up on different days, identical results are produced. This includes not only base pressure and injected volume in each cycle, but also individual pressure spikes in the recorded trace, which may at first appear to be random. After-injection and temporary conditions of vapor pressure are also very repro-

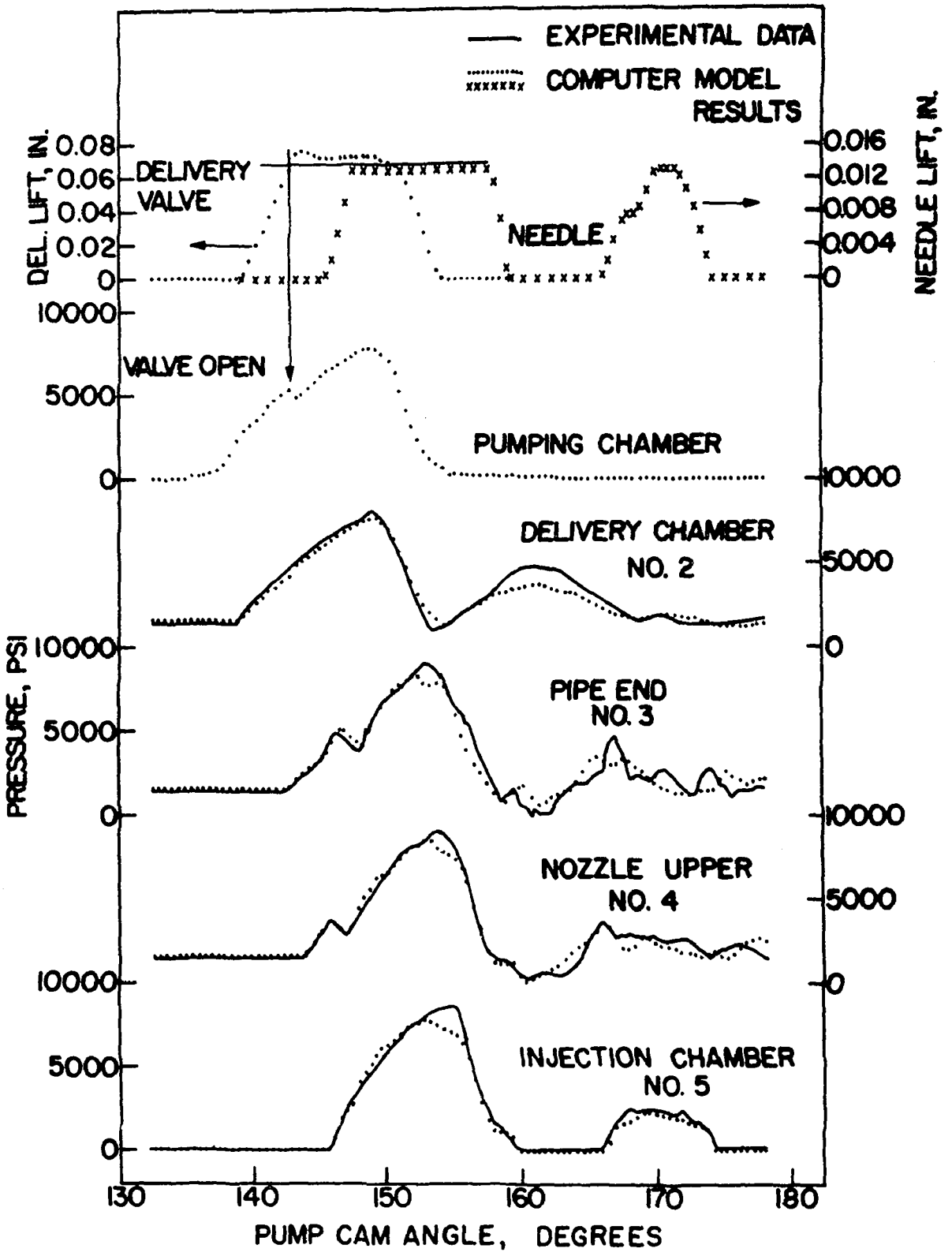

Fig. 8 - Comparison of injection system hydraulic characteristics - experimental and computer results, 800 rpm pump speed and 0.509 rack micrometer (0.1910 lb fuel injected/minute)

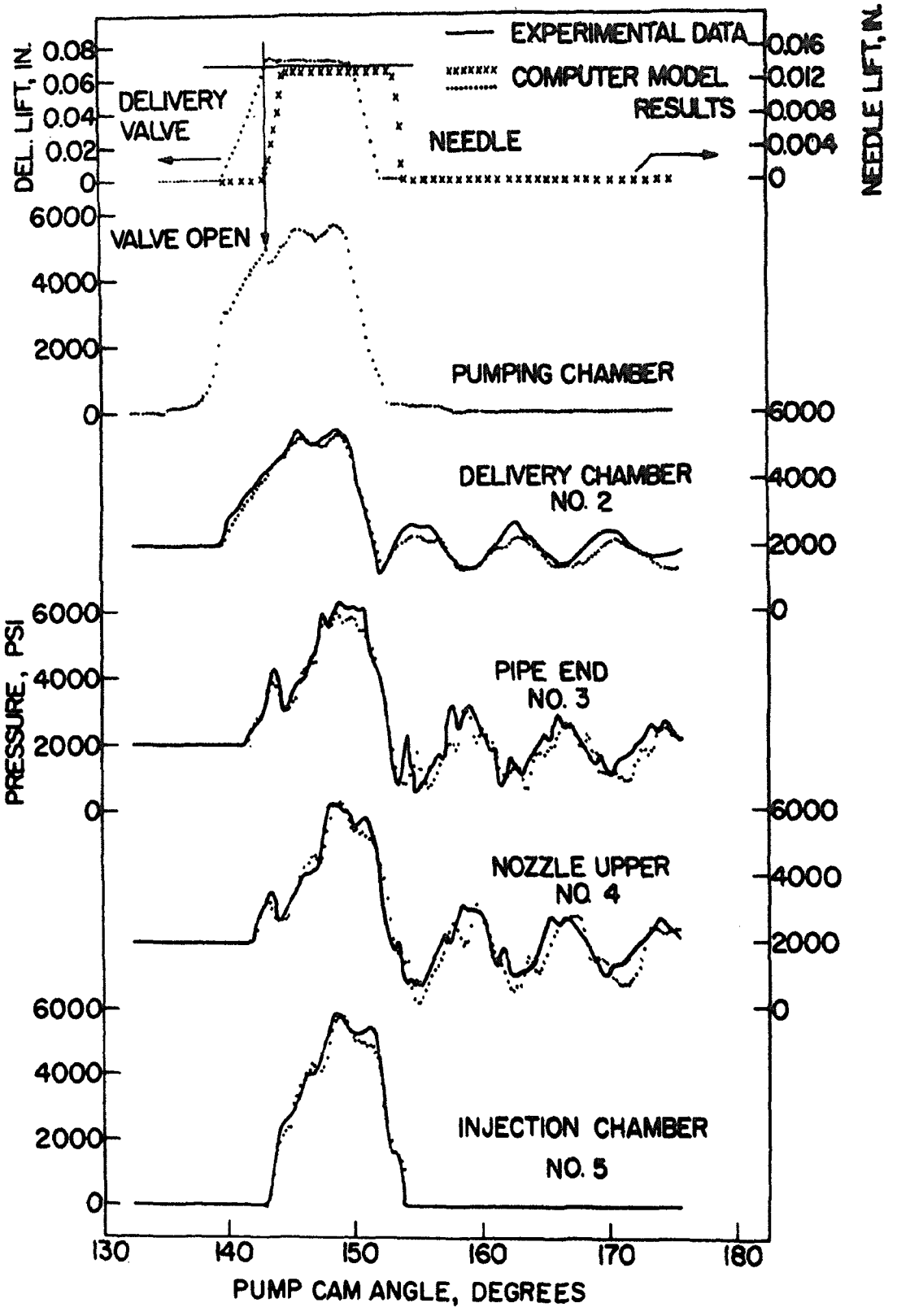

Fig. 9 - Comparison of injection system hydraulic characteristics - experimental and computer results, 400 rpm and 0.509 rack micrometer (0.0968 lb fuel injected/minute)

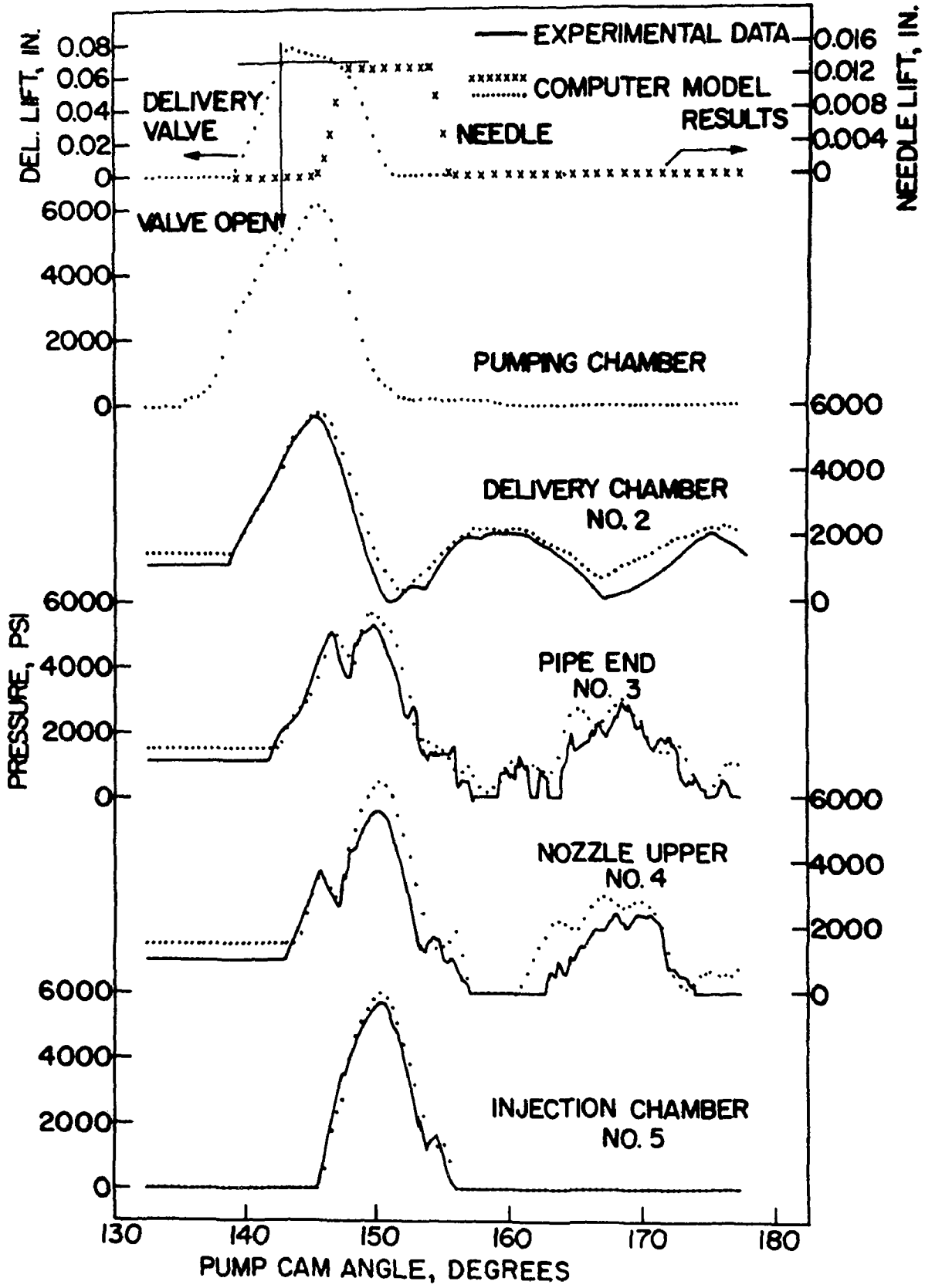

Fig. 10 - Comparison of injection system hydraulic characteristics - experimental and computer results, 800 rpm and 0.675 micrometer (0.0818 lb fuel injected/minute)

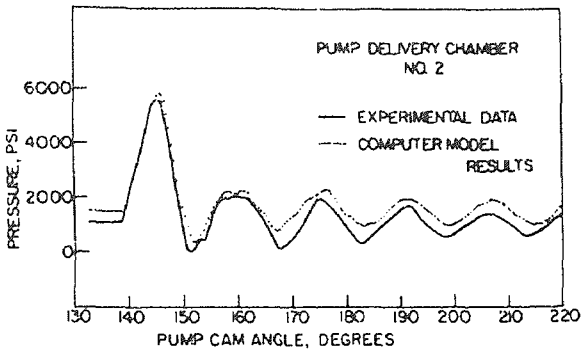

Fig. 11 - Comparison of pressures in pump delivery chamber, experimental and computer results for a large cam angle

Table 1 - Comparison of Base Pressure* and Injected Fuel Quantity Obtained from Experiment and Computer Model

	Figs. 7 and 8	Fig. 9	Figs. 10 and 11
Speed, rpm	800	400	800
Micrometer setting, in. Range: 1 in. (no load) to 0 in. (full load)	0.509	0.509	0.675
Experiment, vol/cycle, in.^{3}	0.00796	0.00805	0.00340
Base pressure, psi	1400	–	1100
Simulation, vol/cycle, in.^{3}	0.00789	0.0084	0.00357
Base pressure, psi	1600	2000	1490

*The base pressure is the residual fuel-line pressure between successive injections.

ducible if these are traits peculiar to the particular operating condition.

COMPARISON–EXPERIMENTAL AND ANALYTICAL DATA

Comparisons are presented for three different test conditions. Fig. 8 displays computer results of pressure variations at five locations, as well as pump delivery valve and nozzle needle motion, all as a function of cam angle. Experimental data are also shown for corresponding transducer locations. These are the same data as displayed in Figs. 6 and 7 and represent the portion of the cycle when fuel injection occurs. Figs. 9 and 10 provide comparisons of two different test conditions: 400 rpm and rack micrometer of 0.509 in., and 800 rpm and rack micrometer of 0.675 in., respectively. A comparison of experimental and simulated pressure in the pump delivery chamber for a larger pump cam angle is shown in Fig. 11. These results are from the same test as those shown in Fig. 10. Additionally, Table 1 provides a comparison of the base pressure and fuel injected for each of the reported cases.

It is observed that the analytical model produces a reasonably accurate reproduction of the pressure-time response recorded from the experimental test setup. By reference to Fig. 8, a cause and effect study of the response during the injection period is possible. For example, the delivery chamber pressure rises while the delivery valve opens, and drops with the delivery valve when the plunger helix is uncovered. The needle valve opens after the nozzle upper chamber pressure exceeds the injector opening pressure of 3000 psi; the nozzle upper chamber pressure drops temporarily and the injection chamber pressure begins to rise at the instant of needle opening; nozzle pressures and needle motion during after-injection are easily correlated; etc. Such features as the time delay in pressure wave travel from pump to injector needle, wave reflection phenomena, pressure peaking at the needle, delivery valve over-shoot before stabilizing at a particular opening during delivery, needle lift motion to the limit position and holding during injection, after-injection 10-15 camshaft rotation deg after the cessation of the primary injection, as well as many other relevant phenomena are identifiable with careful study of these figures.

DISCUSSION

The general agreement in pressure response between experimental and simulation results generates some confidence in the analytical model. The reproducibility of experimental results produces a similar confidence in the reliability of the measured quantities. Various features relative to both the equipment and simulation are discussed in some detail.

MASS CONTINUITY - The experimental equipment provided a measurement of the fuel pumped and the fuel injected over a number of cycles during the test. The leakage that occurs at the needle in the injector and at the pump plunger is available by subtraction. In most tests this leakage was less than 3% of the volume injected. The computer model similarly accumulated the volume pumped and injected during the cycle and also the leakage volume. A good check on the reliability of a numerical simulation of an unsteady fluid flow problem is the gross continuity balance. In acceptable simulations of test runs with this model, the continuity was within 4.0%. The leakage volume per cycle is one of the important variables to be accurately modeled, if a good pressure agreement is to be expected. An additional check on the agreement between experiment and model is provided in the mass continuity comparison, Table 1, where it is seen to be less than 4.5%.

BASE PRESSURE - The initial pressure in the delivery pipeline in the system is recognized as one of the important variables and, unfortunately, a difficult value to measure. The establishment of an identifiable reference pressure is not easy in the operating condition. If vapor pressure is reached and can be identified it provides a suitable reference. In this apparatus, the strain gage mounted on the delivery pipe was used to establish this residual pressure. It is believed that the accuracy of this reading is likely within 300 psi.

In the computer model an initial base pressure was used to

start each run. Initially this was always the experimental value. Following the simulation, an evaluation of the elastic energy stored in the system is possible by use of the pressures along the pipeline, in the pump delivery chamber, and in the injector. If the elastic energy stored after the cessation of fuel supply and injection is different from the initial value, a new value of base pressure is estimated and the run is repeated. No more than one extra trial was needed to satisfy this condition, and normally the correction was less than 300 psi. It is to be noted that discrepancies in the initial and final base pressures give rise to continuity errors in the simulation.

WAVE PROPAGATION VELOCITY - The effective bulk modulus of elasticity of the fluid in the initial operating condition was evaluated by use of a measurement of the wave propagation velocity from the actual experimental recordings. The variation of the modulus with pressure was considered in accordance with the literature (14). This refinement produced a wave speed variation between 4017 and 4391 fps in the pipeline. Minor improvements in the timing of pressure peaks were made with this modeling as compared with a constant wave speed or bulk modulus.

DISTRIBUTED FRICTION - Viscous losses in the system control the rate of attenuation of the residual waves in the system following the primary injection, and exhibit only a modest influence on the initial pressure and discharge waves. The variation of the friction factor with Reynolds number in the model is not considered too important, although too large a pipeline resistance parameter drastically alters the response pattern.

DISCHARGE COEFFICIENTS - Each of the valve ports, orifices, and flow passageways requires a discharge coefficient in the simulation that is a function of a number of parameters, some of which are time dependent. The magnitude of this value at some of the locations is very critical in the production of a reasonable simulation. Computational results seemed to be most sensitive to the values used at the injector nozzle, the needle passage to the injection chamber, and the pump delivery valve. These same values are also difficult to estimate on the basis of information in the literature due to the unusual geometric configuration. Steady-state measurements on this system were not attempted. Best results in the simulation have been obtained by use of values calculated, where possible, from the measured transient pressure response. Values ascertained in this manner have been reasonably constant in the various experiments. Constant values have been used in all past simulations.

VAPOR PRESSURE - When vapor pressure is reached in the pipeline, a vapor pocket develops and subsequently collapses. This phenomenon is discernible in transducer records by a flat bottom pressure trace for a short period of time. The computer model reproduces the same condition by not permitting the pressure to drop below vapor pressure. A local cavity is allowed to develop and its size is computed by a mass continuity balance. When the cavity goes to zero, the normal computations resume with conditions of a homogeneous fuel at the former cavity location.

SOLUTION OF DYNAMIC EQUATIONS - The handling of the dynamic equations that describe the motion of the pump delivery valve and the nozzle needle, and the fluid compressibility in lumped volumes, is most critical to a satisfactory system simulation. The response time of these features is extremely rapid. Hamming's modified predictor-corrector method was found to be the most successful procedure in this simulation.

CONCLUSIONS

The analytical model can be confidently used to study various system configurations and proposed design changes. The computer simulation can serve as an excellent design tool with which to perform many additional parametric studies to ascertain the influence of changes in various geometric and mechanical variables. The analytical model can assist in understanding fuel injection systems, and its use can shorten the development time required to improve fuel injection characteristics which may lead to improved combustion and reduced exhaust emissions. It will be apparent that the model described can be most easily adapted to systems similar to the one used in this work. We believe the modeling techniques outlined can be applied effectively to other types of injection systems.

ACKNOWLEDGMENT

This investigation was supported by United States Public Health Service Research Grant No. AP00835, from the National Air Pollution Control Administration. The work was also assisted by research funds provided by the Chevron Research Co. The valuable contributions of graduate students Bela Petry, Arthur Bauer, and S. Onyegegbu are also appreciated.

NOMENCLATURE

A	= Pipe cross-sectional area, or area of opening at orifice
a	= Wave propagation velocity
C_d	= Discharge coefficient
D	= Pipe diameter
d	= Subscript, refers to pump delivery chamber
f	= Friction coefficient at valve or needle
f	= Darcy-Weisbach friction factor
f	= Subscript, refers to pump feed chamber
g	= Acceleration of gravity
i	= Subscript, refers to injector chamber
K	= Bulk modulus of elasticity
k	= Spring force
l	= Subscript, refers to nozzle lower chamber
m	= Mass of valve or injector needle
n	= Subscript, refers to injector needle
p	= Pressure
p	= Subscript, refers to pump chamber

Q	=	Volumetric flow rate
r	=	Spring stiffness
S	=	Valve or needle displacement
t	=	Time
u	=	Subscript, refers to upper nozzle and delivery chamber
V	=	Velocity
$\forall$	=	Volume of fluid enclosures in pump and injector
v	=	Subscript, refers to delivery valve
W, X, Y, Z	=	Subscripts, refer to positions in the x-t plane
W	=	Weight of valve or needle
x	=	Distance
Zd	=	Subscript, refers to instantaneous flow in delivery pipe at pump delivery chamber
Zs	=	Subscript, refers to instantaneous flow in supply pipe at pump feed chamber
Zu	=	Subscript, refers to instantaneous flow in delivery pipe at injector
γ	=	Specific weight of fluid

REFERENCES

1. S. J. Davis and E. Giffen, "Injection, Ignition, and Combustion in High Speed Heavy Oil Engines." Proc. Instn. of Automobile Engrs., (March 1931) p. 399.

2. Kalman J. De Juhasz, "Graphical Analysis of Transient Phenomena in Linear Flow." Jrl. Franklin Inst., (April-June, 1937), pp. 463, 643, 655.

3. E. Giffen and A. W. Rowe, "Pressure Calculations for Oil Engine Fuel-Injection System." Proc. Instn. Mech. Engrs., London, Vol. 141 (1939) p. 519.

4. B. E. Knight, "Fuel Injection System Calculations." Proc. Inst. Mech. Engrs. (A.D.), No. 1 (1960-1961).

5. P. I. Becchi, "The Analytical Investigation of Phenomena Concerning the Fuel Injection in Fast Diesel Engines, Carried out at Design Stage by Means of the Electronic Computer." Tech. Bulletin, Fiat, Vol. XV, No. 2 (April 1962).

6. G. W. Brown and H. McCallion, "Simulation of an Injection System with Delivery Pipe Cavitation Using a Digital Computer." Proc. Instn. Mech. Engrs., London, Vol. 182 (1967-1968) p. 206.

7. J. A. Stone, "Discharge Coefficients and Steady-State Flow Forces for Hydraulic Poppet Valves." Jrl. of Basic Eng., Vol. 82 (1960) p. 144.

8. E. Van Walwijk, R. Van der Graaf, and J. K. M. Jansen, "Berekening Van brandstofinspuitsystemen Voor dieselmotoren." Werktuig-En Scheepsbouw, May 10, 1969, W 95.

9. Frank Kreith and Raymond Eisentadt, "Pressure Drop and Flow Characteristics of Short Capillary Tubes at Low Reynolds Number." ASME Trans. 56, 1956.

10. A. Lichtarowicz, R. K. Duggins, and E. Markland, "Discharge Coefficients for Incompressible Non-Cavitating Flow Through Long Orifices." Jrl. Mech. Engr. Science, Vol. 7, No. 2 (1965).

11. A. G. Gelalles, "Coefficients of Discharge of Fuel Injection Nozzles for Compression-Ignition Engines." National Advisory Committee for Aeronautics Tech. Report No. 373 (1931).

12. P. Henrici, "Elements of Numerical Analysis." New York: John Wiley & Sons, Inc., 1964.

13. J. B. Maxwell, "Data Hand Book on Hydrocarbons; Application to Process Engineering." New York: D. Van Nostrand Co., Inc., 1950.

14. W. A. Wright, "Prediction of Bulk Moduli and PVT Data for Petroleum Oils." ASLE 47 AM 7B-1, May 1-4, 1967.

15. V. L. Streeter and E. B. Wylie, "Hydraulic Transients." New York: McGraw-Hill Book Co., 1967.

16. W. Ralston and H. S. Wilf, "Mathematical Methods for Digital Computers." New York: Wiley & Sons, 1960, pp. 95-109.

17. A. Bassi, "Experimental Investigations into Diesel Injection Systems." Sulzer Research No. 1963.

18. American Bosch Corp., "Fuel Injection and Controls for Internal Combusion Engines." 1963 and New York: Simmons Boardman Publ. Corp., 1962.

This paper is subject to revision. Statements and opinions advanced in papers or discussion are the author's and are his responsibility, not the Society's; however, the paper has been edited by SAE for uniform styling and format. Discussion will be printed with the paper if it is published in SAE Transactions. For permission to publish this paper in full or in part, contact the SAE Publications Division and the authors.

Society of Automotive Engineers, Inc.
TWO PENNSYLVANIA PLAZA, NEW YORK, N.Y. 10001

16 page booklet. Printed in U.S.A.

Fleet Week 73

FLEET OWNER

MOTOR & EQUIPMENT MANUFACTURERS ASSN

SOCIETY OF AUTOMOTIVE ENGINEERS, INC.
Two Pennsylvania Plaza, New York, N.Y. 10001

Analysis and Control of Transient Flow in the Diesel Injection System Part I – The Analytical Control Method

Mohamed F. El-Erian, E. Benjamin Wylie, and Jay A. Bolt
University of Michigan

SOCIETY OF AUTOMOTIVE ENGINEERS

Combined Commercial Vehicle Engineering & Operations and Powerplant Meetings
Chicago, Ill.
June 18-22, 1973

730661

TABLE OF CONTENTS

Abstract . . . . . .
Comparisons of Experimental Data and Simulation Program Results . . . . . .
Average Elastic Energy – The Control Parameter . . . . . .
Description of the Design Method on the Pipe Characteristic Plane . . . . . .
Effect of the Injection System Average Elastic Energy Function on the System Transient Pressures . . . . . .
Average Elastic Energy Release Via Additional Control Valve . . . . . .
Average Elastic Energy Release Via the Pump Spill Port . . . . . .
Conclusions . . . . . .
Nomenclature . . . . . .
Acknowledgment . . . . . .
References . . . . . .
Appendix . . . . . .

Copyright ©Society of Automotive Engineers, Inc. 1973
All rights reserved.

730661

Analysis and Control of Transient Flow in the Diesel Injection System Part I – The Analytical Control Method

Mohamed F. El-Erian, E. Benjamin Wylie, and Jay A. Bolt
University of Michigan

THE OPERATION of the injection system of a diesel engine is of critical importance since it has a major influence on the combustion process in the engine. Optimal operating conditions are particularly important in view of current air pollution problems. Also, present uses of the diesel engine are somewhat limited due to current operating combustion characteristics.

One of the most persistent injection system problems is related to wave phenomena in the high-pressure line between the pump and nozzle assembly of the most popular type of injection system. These pressure waves commonly result in a secondary opening of the fuel injection nozzle following the normal injection which is referred to as after-injection. This results in reduced engine performance and increased emissions.

Bradbury (1)* showed that after-injection invariably occurred at conditions of simultaneous high engine speed and load. In addition, his studies on the relation between the

*Numbers in parentheses designate References at end of paper.

ABSTRACT

The increasing requirements imposed on diesel engine manufacturers have required the study of fuel injection system faults and the development of means to eliminate them. Until now, improved injection system characteristics have been obtained by experimental trial-and-error procedures. These procedures, however, have proved to be inconvenient, tedious, and have had limited success in eliminating system faults such as after-injection. This is mainly because the transient nature of the injection process requires a more thorough study of the system time-varying parameters.

In this paper the residual transients which cause after-injection are analytically investigated. The control of these transients required specification of some system parameter. The rapidly varying nature of the system pressures and flows prevented the use of these variables as control parameters. On the other hand, the average instantaneous elastic energy stored in the system was found to be a well-behaved function of time and was therefore selected as the control parameter.

A design procedure to control after-injection was formulated. In this procedure, design changes required to achieve improved system characteristics were obtained by specification of the average elastic energy function. Two design changes were considered. These included the design of an additional control valve in the pump delivery chamber and the redesign of the pump spill port. The design techniques used in the control method are described in this paper, while the application, results, and experimental verifications are given in a companion paper.

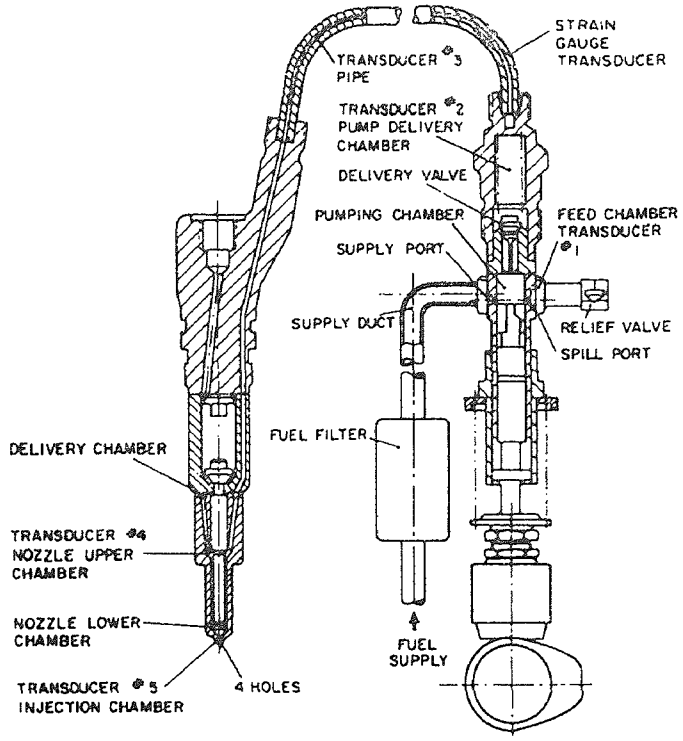

Fig. 1 - Schematic representation of diesel injection system and points of pressure measurement

brake specific fuel consumption and break mean effective pressure indicated the need for large injector holes to achieve large output, and that small holes were more adequate for part-loads. He concluded that small holes are preferred over the whole range if it is possible to eliminate after-injection at high outputs.

Similar information was obtained by personal communications with A. C. Rosselli (2): "We have consistently found that high injection pressures with small holes tend to give superior performance. The effect of very high injection pressures on smoke tend to be especially significant." Furthermore, it is shown in Ref. 3 that after-injection considerably increases unburned hydrocarbons emissions.

Mansfield (4) summarized the problem as, "It is difficult if not impossible, for a pump to perform satisfactorily on a heavy-duty engine under all conditions of speed and load, and that the high rates of pressure change, which must occur in all injection systems, lead to secondary injection."

Many experimental trial-and-error methods have been used to control this phenomenon. These include studies of the effect of the nozzle injection area and the delivery pipe diameter or length among other parameters. Limited success is expected from using these methods due to the fact that these design changes are time-invariant and hence do not suit the transient nature of the problem. More success may be realized by design alterations of the time-varying parameters of the system. An example of such a parameter is the instantaneous area of the spill port during the spill period.

Recently Dolenc and Lees (5) and Lustgarten and Dolenc (6) used a pump plunger with a stepped helix which provided a throttling effect during the early part of the fuel spill period. Their experimental results showed that the modified system provided improved performance compared with the original system. This was evidenced by less after-injection and reduced cavitational damage.

Prior to 1960, theoretical studies of objectionable transients in hydraulic systems were limited due to the requirement of lengthy mathematical computations. By introducing a certain number of simplifying assumptions, simple diesel injection systems were analyzed and design variations tried until acceptable performance was achieved. Since 1960 a number of injection simulation computer programs have been developed (7-9); however, none of the published literature in this field indicates a use of the concept of design synthesis.

In related areas of fluid mechanics a procedure referred to as "valve stroking" (10) has been developed and applied to various water, oil, and natural-gas systems. In this procedure the desired time-varying flow and pressure relations are specified at a section in the system, and computations are performed to yield the required behavior at other positions in the system. Boundary conditions may then be imposed to accomplish the desired conditions. This synthesis procedure is a more direct approach to design changes in transient fluid flow problems and leads to sophisticated control techniques not easily attainable by standard simulation methods.

Although direct application of the valve-stroking techniques to the diesel injection system proved unsuccessful, the calculation concepts were applicable. Failure of the direct

Table 1 - Résumé of Testing Conditions Used to Compare with the Simulation Program and Used to Study the After-Injection Phenomenon

Test No	Speed, rpm	Rack Micrometer Setting, in*	Total Fuel Injected, lb/min	Base Pressure, psi	C_t**, in^2	After-Injection, lb/min	% After-Injection of Total Injection
1	800	0.509	0.191	1400	0.000178	0.0510	26.70
2	365	0.608	0.054	1300	0.000127	0.0055	10.19
3	405	0.350	0.148	2000	0.000126	0.0343	23.18
4	700	0.426	0.216	2500	0.000128	0.0796	36.85

*Rack micrometer setting: $in = 1 - \frac{\text{test load}}{\text{maximum load}}$

**$C_t = cd \cdot A_h$ where A_h is the area of nozzle injection holes and cd is a coefficient of discharge.

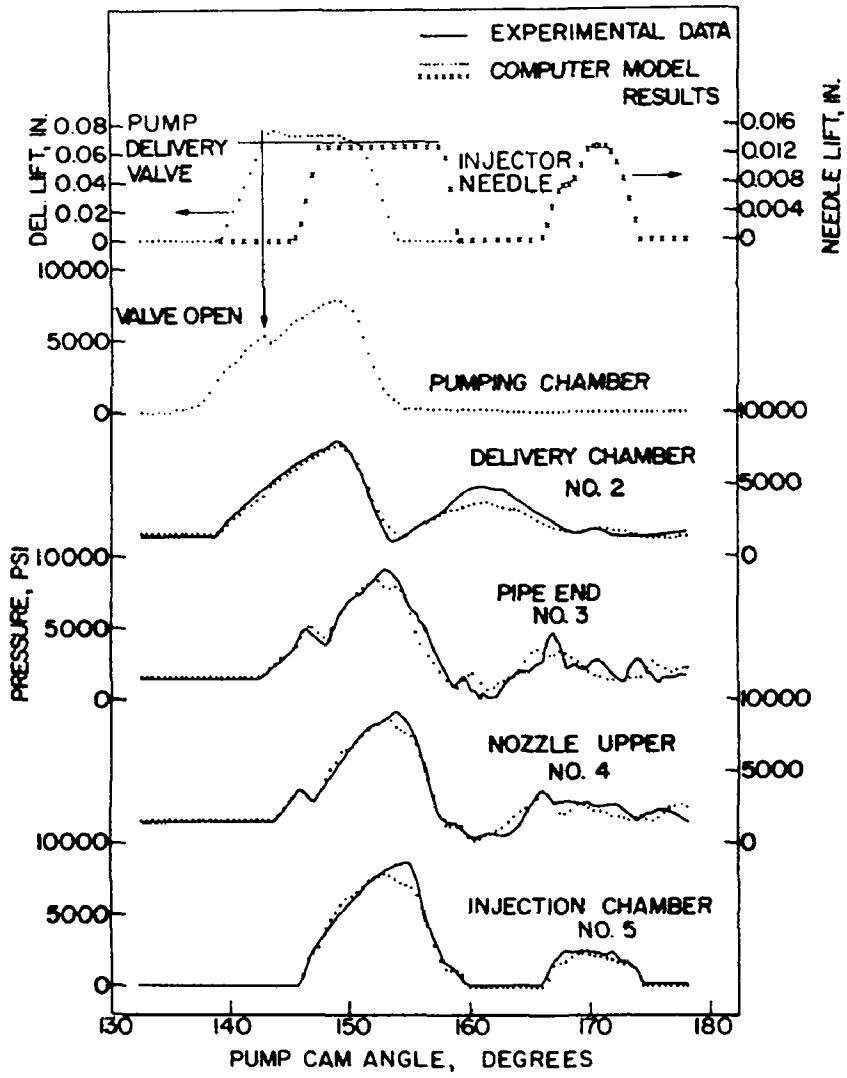

Fig. 2 - Comparison of injection system hydraulic characteristics–experimental and computer results, 800 rpm pump speed and 0.509 rack micrometer (0.1910 lb fuel injected/min)

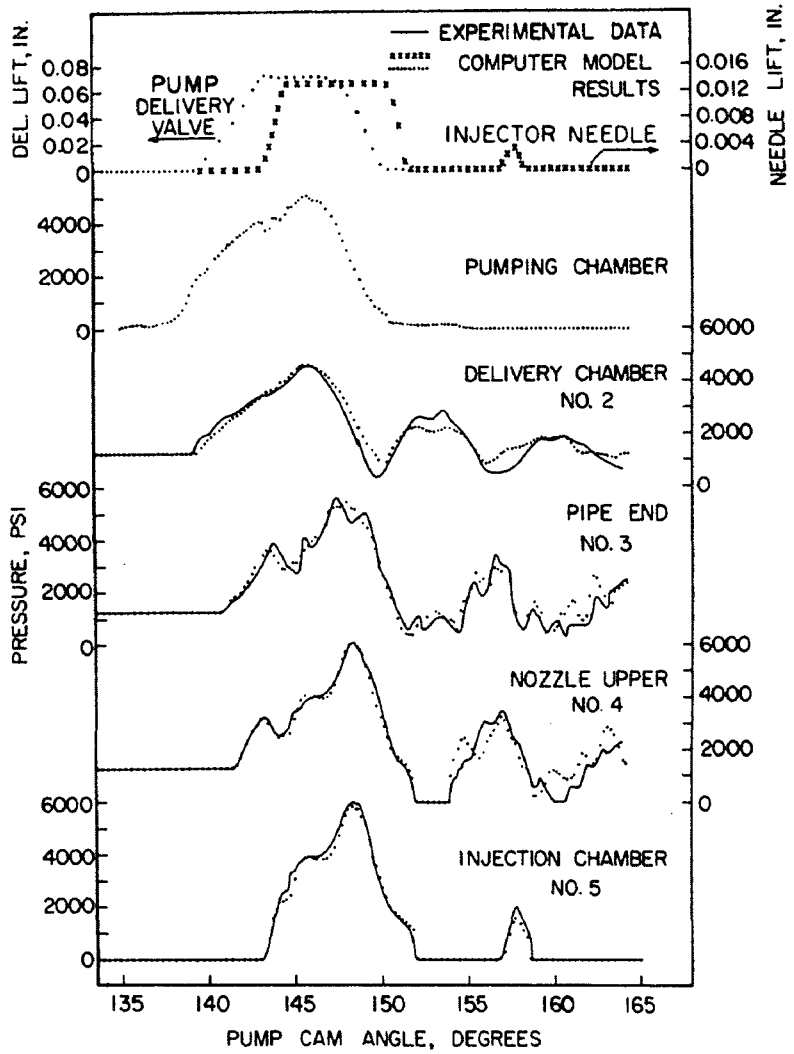

Fig. 3 - Comparison of injection system hydraulic characteristics–experimental and computer results, 365 rpm pump speed and 0.608 rack micrometer (0.054 lb fuel injected/min)

Table 2 - Comparison Between Theoretical and Experimental Results for Data Presented in Table 1 and Figs. 2-5

			Experimental Data		Simulation Results	
Test No.	Speed, rpm	Rack Micrometer Setting, in	Injected Fuel, in ^{3}/cycle	Base Pressure, psi	Injected Fuel, in^3/cycle	Base Pressure, psi
1	800	0.509	0.00796	1400	0.00789	1600
2	365	0.608	0.00493	1300	0.00511	1400
3	405	0.350	0.01218	2000	0.01193	1988
4	700	0.426	0.01029	2500	0.01011	.2430

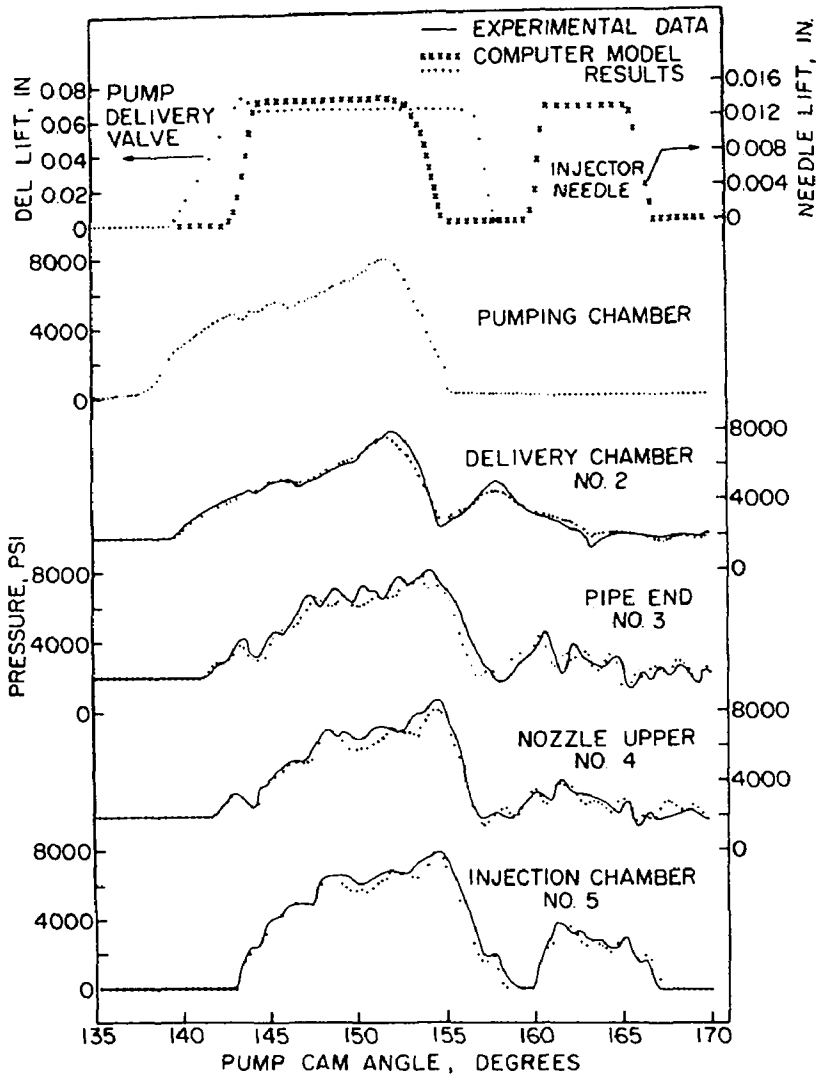

Fig. 4 - Comparison of injection system hydraulic characteristics–experimental and computer results, 405 rpm pump speed and 0.350 rack micrometer (0.1480 lb fuel injected/min)

application was due to the passive type elements in the system which respond to internal driving forces rather than to externally forced conditions. Additionally, the rapidly varying nature of both pressure and flow in the system made specification of these variables difficult, if not impossible. This led to the seeking of a design parameter which did not exhibit erratic behavior. As discussed later, the system average elastic energy was found to be a suitable parameter.

The purpose of this paper is to describe an analytical control method which was developed and used with a theoretical simulation program to improve injection characteristics and to determine needed design changes. Several cases, each including the undesirable phenomenon of after-injection, are theoretically simulated and compared with actual experimental data. Both the control parameter and the theoretical control technique are described and combined in a design procedure. The design procedure is used to study the effect of the control parameter on the injection characteristics in relation to two design changes, namely, the use of an additional pump control valve and the redesigning of the pump spill port. The usefulness of this procedure is illustrated by its ability to eliminate after-injection in the studied cases. Computer results of design changes needed to eliminate after-injection are presented in part II of this paper. These results are confirmed by using the simulation program. Experimental data are also given to verify a pump spill port redesign which resulted in eliminating after-injection.

COMPARISONS OF EXPERIMENTAL DATA AND SIMULATION PROGRAM RESULTS

The experimental equipment and the simulation program used in this study are described in Refs. 9 and 11. A schematic representation of the injection system and the points of pressure measurements is illustrated in Fig. 1. In addition, the injection system equations are summarized in the Appendix.

Several experiments have been conducted to cover a wide

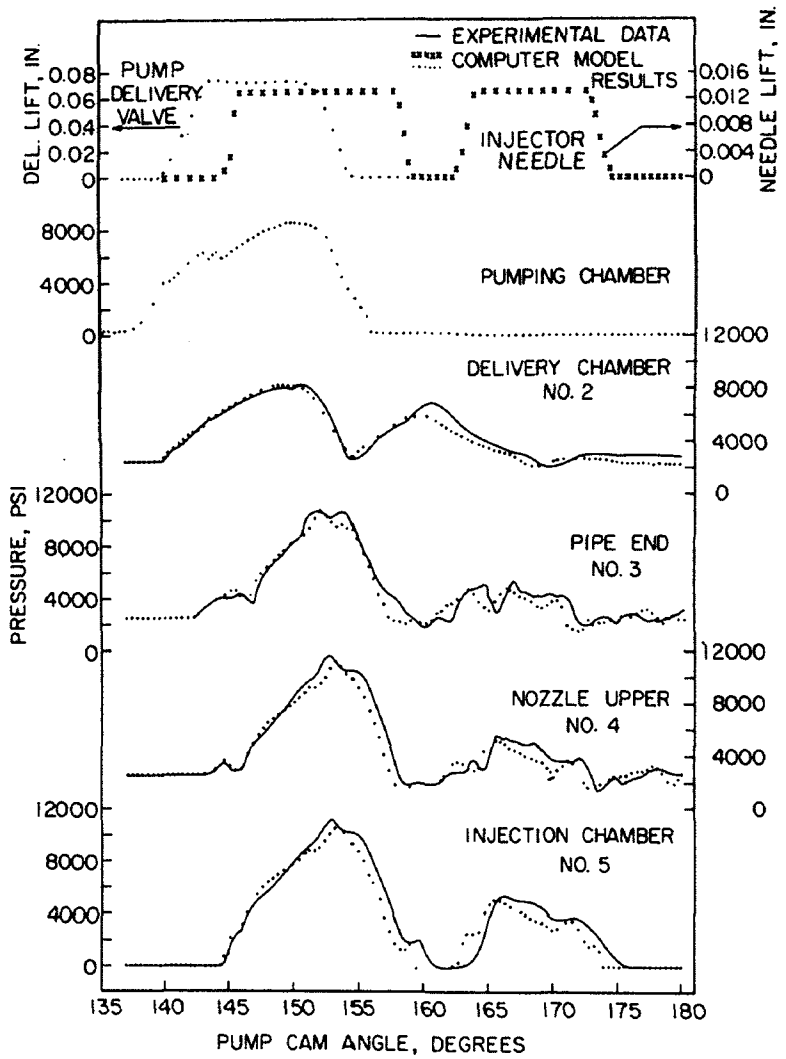

Fig. 5 - Comparison of injection system hydraulic characteristics—experimental and computer results, 700 rpm pump speed and 0.426 rack micrometer (0.216 lb fuel injected/min)

range of speed and load conditions. Four of these test runs, with different amounts of after-injection, are summarized in Table 1. Each test is identified by pump cam speed, a fuel rack setting, the total amount of fuel injected, the pipe base pressure which is the residual pressure remaining in the pipeline between cycles, and the coefficient C_t which is the product of the total nozzle injection hole area and the coefficient of discharge. In addition, the amount of after-injection and its percentage to the total injection are given in Table 1.

Tests 2, 3, and 4 were run at a lower injection hole area than test 1. This was necessary to produce after-injection at various speed and load conditions so that this phenomenon could be simulated and then theoretically investigated. Tests 2, 3, and 4 were chosen to represent low-, medium-, and high-speed and load conditions, respectively. It is seen from the table that a simultaneous increase of speed and load results in an increase of after-injection.

Comparisons between experimental data and results from the simulation program for the four test conditions listed in Table 1 are presented in Figs. 2-5. Comparisons of transient pressure traces are possible at four locations: the delivery chamber, the pipe end, the nozzle upper chamber, and the injection chamber. Also, theoretical results for the pressure variation at the pumping chamber and motion of the pump delivery valve and nozzle needle are included in the same set of figures. All the injection system variables are presented as functions of the pump cam angle for the portion of the cycle in which fuel injection occurs. The computer model results, together with the experimental data for the system residual pressure and the injected fuel for each of the four cases considered, are listed in Table 2. The favorable comparisons between the results from the analytical model and the experimental data generate confidence in the underlying assumptions and techniques used in developing the model.

A cause-and-effect study of the injection system response

is possible by examining any of the presented cases (Figs. 2-5). For example, the pressure in the pumping chamber begins to rise slowly because the ports are still partly uncovered. When the ports are covered, the pressure rises rapidly. The pressure in the pump delivery chamber rises when the delivery valve opens and drops with the delivery valve closing. The nozzle needle opens after the pressure in the nozzle upper chamber exceeds the injector-opening pressure of 3000 psi. This causes the nozzle upper chamber pressure to drop temporarily and the injection chamber pressure to begin to rise at the instant of needle opening. The needle motion and nozzle pressure are easily correlated for after-injection. The wave reflection phenomenon and the time delay in pressure wave travel are made clear by comparing pressures at different locations.

AVERAGE ELASTIC ENERGY–THE CONTROL PARAMETER

In this study, the term average elastic energy is used to define the average pressure stored in the injection system at an instant of time. It should be noted that this pressure has the units of energy per unit displaced volume at the boundaries. Two examples are given to illustrate this definition. First, a moving frictionless piston in a liquid-filled cylinder exerts work on the liquid. This energy is stored in the elastic deformation of the liquid and could be used to drive the piston back to its initial position. The second example is drawn from unsteady liquid flow in a frictionless pipe. In this example, elastic energy is stored in a liquid column due to the compression of the column. This energy is released as kinetic energy by the expansion of the column.

The dotted system in Fig. 6 is used to calculate the injection system average elastic energy. This system includes the fluid in the pump delivery chamber, in the injector delivery, upper and lower chambers, and in the delivery pipeline. The terms P and L_{TOT} are defined in Fig. 7. In this figure, L_{PUMP} and L_{INJ} are equivalent lengths to match the corresponding volumes in the pump and injector, respectively. The average elastic energy at an instant is calculated in the manner described in Figs. 6 and 7.

During each cycle the pump adds energy in the form of flow work which is temporarily stored in the system as elastic energy. Part of this energy is released at the injection nozzle during the injection period. If excessive uncontrolled elastic energy remains in the system following the closure of the pump delivery valve, it will be released at the nozzle resulting in after-injection.

The average elastic energy together with pressure in the pump delivery chamber and nozzle upper chamber for test 1 (Table 1) are displayed in Fig. 8. All the traces begin at the point when the spill port begins to open. In region I, the average elastic energy drops because of spilling at the pump spill port plus the energy release due to injection at the nozzle. Region II begins when the delivery valve closes. The energy drop in this region is due to injection at the

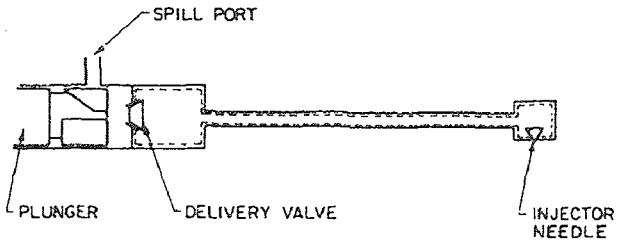

$$\text{AVERAGE ELASTIC ENERGY} = \frac{\int p\,dx}{L_{TOT}}$$

Fig. 6 - Schematic representation of system used to calculate the average elastic energy

nozzle only. Region II ends when the nozzle needle begins to close while region III coincides with the period of needle closure. For this region slight increase in elastic energy might occur due to the effect of work done by the needle compressing the fuel during its downward motion. When the needle finally closes, the nozzle upper chamber pressure is lower than the needle-opening pressure. However, the intermediate elastic energy in region IV is high, thus causing the pressure at the nozzle upper chamber to increase as the pressure wave reflects in the closed system. When this pressure reaches the needle-opening pressure, the needle opens and the system elastic energy drops during region V. Later on, the upper chamber pressure drops below the needle-closing pressure and the needle closes. At this point, the system elastic energy finally reaches the residual energy. The elastic energy stays constant during region VI until the next cycle begins.

The average elastic energy trace in Fig. 8 gives a better understanding of the after-injection phenomenon. A study of a number of similar cases led to the conclusion that the manner in which the energy is released during the spill period (region I) largely regulates the behavior of the residual transients in the injection system. For example, a rapid energy drop in region I causes a rapid closing of the delivery valve which means a higher intermediate energy and therefore an increased after-injection. On the other hand, a very slow drop during the spill period leads to prolonged injection periods and low-pressure injection. Thus one possible approach to the reduction of undesirable transients in the system is to focus attention on the controlled release of the average elastic energy.

DESCRIPTION OF THE DESIGN METHOD ON THE PIPE CHARACTERISTIC PLANE

The investigation of a specific case of after-injection begins with recording experimental data of the actual test condition. Then the simulation program is used to simulate this condition. Comparisons between theoretical results and experimental data of four cases of after-injection were presented in Figs. 2-5. The design program presented in this section serves the purpose of finding means to eliminate after-injec-

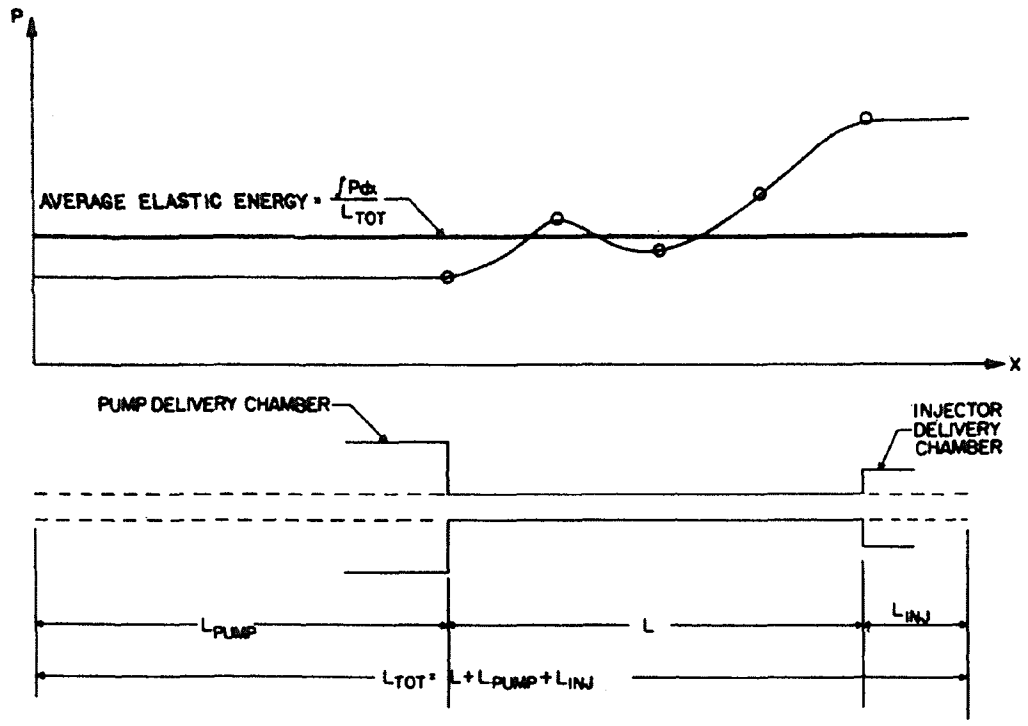

Fig. 7 - Sketch showing the method for calculating the injection system average elastic energy

tion. This is achieved by utilizing a controlled release of the stored elastic energy in the system. The resulting alterations in pressure and flow patterns are calculated and translated into feasible design changes using the design program.

Fig. 9 represents the pipe characteristic plane (x-t plane). An instant of time is represented by a horizontal line while a vertical line represents a specific location along the pipe. The line AJ represents the location of the pump delivery chamber, and the line BI represents the location of the injector delivery chamber. Line ED represents the instant of time at which the negative wave, resulting from the uncovering of the pump spill port, reaches the injector. Line HG represents the instant of nozzle needle closing. Three important events characterize the performance of the diesel injection system and are given in Fig. 9: First, the plunger helix begins to uncover the spill port at point C; then the pump delivery valve is totally closed at F; finally, the nozzle needle is totally closed at G. In this figure, the distance AC is the wave travel time and BD is twice the wave travel time.

The design method is illustrated in Fig. 10 which is similar to Fig. 9 but includes more details of the solution procedure. In this figure, the distance between the vertical lines represents a pipe section of length Δx, while the distance between the horizontal lines is the characteristic method time step Δt. The data needed by the design program include a complete description of the injection system geometric configuration and properties. Simulation program results of pressure and flow along the line BD are specified for the design program. Also a control period beginning at point C together with a controlled average elastic energy function are specified. The choice of the length of the control period and the energy function during this period depend on the injection system properties and the choice of the controlling device. Further discussion of this subject will be presented in the next section.

Several regions are given in Fig. 10 to simplify the presentation of the solution method. The solution procedure in region I begins with known pressure and flow conditions at all points along the vertical line BD. Conditions at points lying on another vertical line adjacent to BD are calculated by the use of the pipe characteristic equations (Eqs. A-11 and A-13 in the Appendix) in a manner illustrated by the triangle $Z_1Y_1W_1$. In this triangle, pressure and flow conditions are known at Y_1 and W_1 but are not known at Z_1. It should be noted that Z_1W_1 is the C^+ characteristic line and Y_1Z_1 is the C^- characteristic line. When the conditions at all points lying on a vertical line are calculated, the calculation proceeds to points on the next adjacent vertical line. Calculations in region I end when the pressure and flow at point C are known.

In region II, calculations begin at $t = L/a + \Delta t$. At this instant, pressure and flow conditions are known for all pipe locations except the boundary point W_2. Conditions at this boundary point are calculated by making use of the assumed instantaneous average elastic energy together with an equation from the pipe C^- characteristic line. At $t = L/a + 2\Delta t$, pressures and flows are known at all points except at Z_2 and Z_3. At this point of time, conditions at the interior point

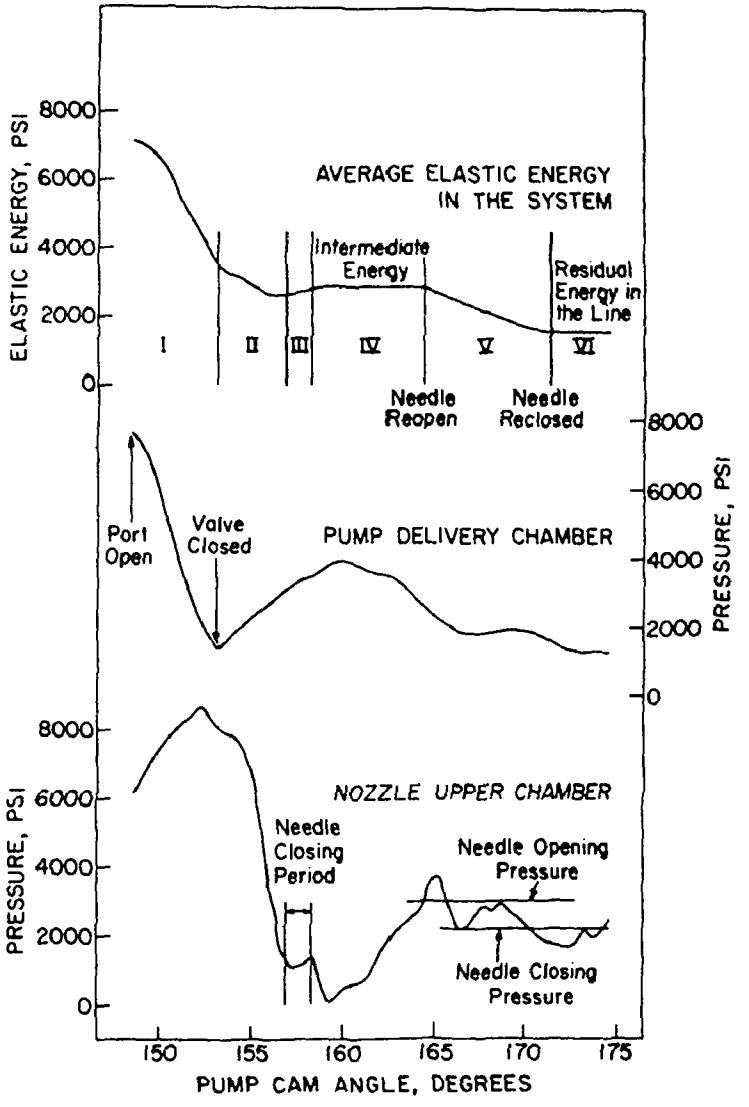

Fig. 8 - Transient pressures and average elastic energy versus pump cam angle for test 1 (Table 1)

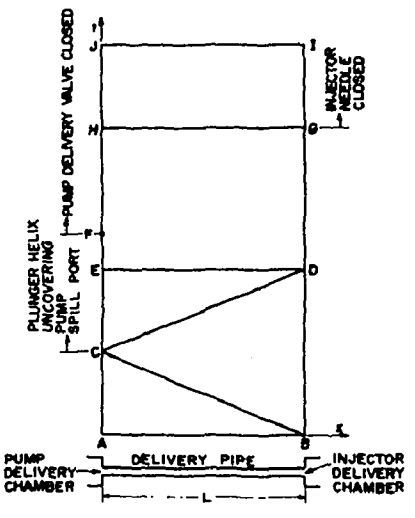

Fig. 9 - Injection system performance on the pipe x-t plane

(Z_2) are calculated by utilizing the known pressures and flows at W_2 and Y_2 together with the pipe characteristic equations along the C^+ line W_2Z_2 and the C^- line Y_2Z_2. Conditions at Z_3 are calculated in the same manner described for W_2. This procedure continues by advancing to the next step, calculating the interior points, and then calculating the boundary point along the line CE. Calculations in this region end by calculating pressures and flows at all points along the horizontal line ED.

Calculations in region III proceed by calculating all pressures and flows at time t prior to calculating these conditions at time $t + \Delta t$. This is done by first calculating the interior points in the same manner previously described for point Z_2 in region II. Then conditions at the injector boundary point along the line DG are calculated by solving the injector equations (Eqs. A-6-A-10) together with the pipe characteristic equation along the C^+ line illustrated by

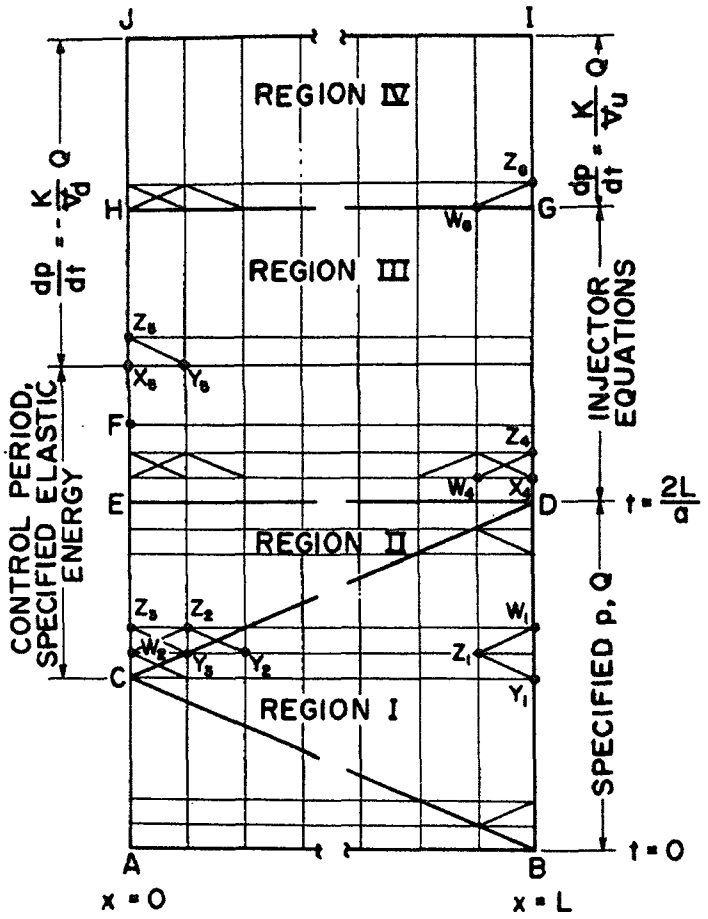

Fig. 10 - Design method on the pipe x-t plane

the line W_4Z_4. Finally the pump boundary point along EH is calculated. During the control period, this calculation is performed in the same manner described for W_2. After the end of the control period, the compressibility equation $dP/dt = -(K/\forall_d)Q$ describes the conditions in the pump delivery chamber and is used together with the pipe C^- characteristic equation to determine the pressure and flow at the pump boundary. This C^- line is illustrated by the line Y_5Z_5. Similarly, the compressibility equation $dP/dt = (K/\forall_u)Q$ relates the pressure and flow in the combined injector chambers after the needle is completely closed. This equation is used together with the pipe C^+ characteristic equation to determine the pressure and flow at the injector boundary in region IV. In this region, the interior points and pump boundary point are calculated in the same manner described for region III. Since the design program objectives are to eliminate undesirable system characteristics (after-injection and cavitation), no provision has been made to simulate these phenomena.

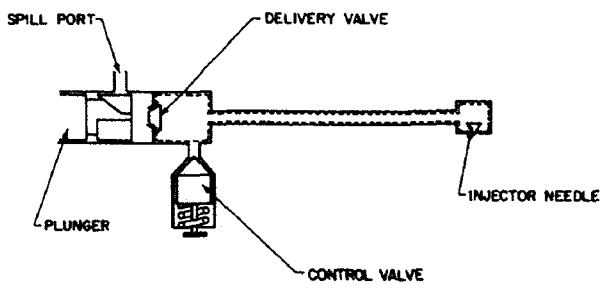

Fig. 11 - Schematic representation of the control valve position

EFFECT OF THE INJECTION SYSTEM AVERAGE ELASTIC ENERGY FUNCTION ON THE SYSTEM TRANSIENT PRESSURES

The above design procedure has utilized a specified average elastic energy function and known initial conditions to calculate the injection system transient pressures. Attention is now given to the determination of an optimum way of specifying this average elastic energy function. In this study,

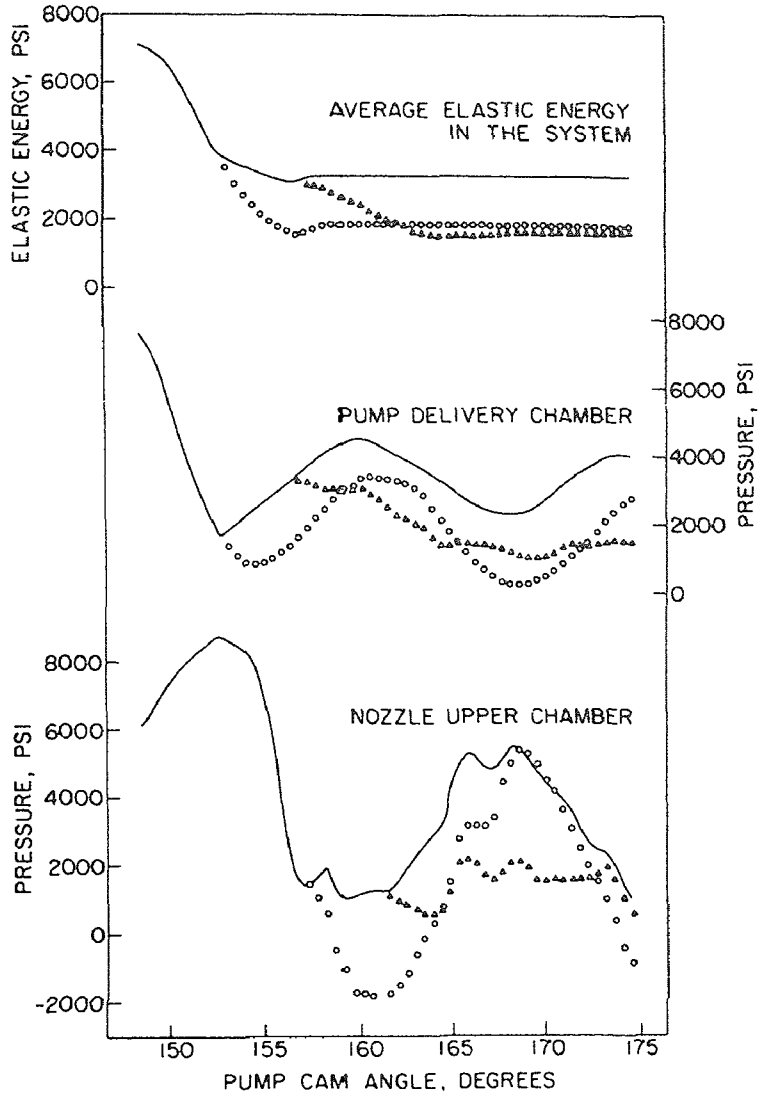

Fig. 12 - Injection system variables versus pump cam angle. Effect of timing the average elastic energy drop. Control valve approach, test 1 (Table 1)

the desired optimum function is defined as the one that will result in damping the residual transient pressures in a way that eliminates after-injection over a desired range of operating conditions without seriously altering the injection pressures during the main injection period and without introducing any undesirable effects (such as cavitation). This definition implies the following:

1. The original average elastic energy function during region I (Fig. 8) should not be seriously altered in order to retain the shape of the injection pressures during the main injection.

2. The injection system stored elastic energy must reach the system original residual energy (Fig. 8) by the end of the control period shown in Fig. 10.

Different objective functions could be defined and utilized equally well to assist in the solution of other types of injection design problems.

In order to physically achieve a desired specified elastic energy function, two design changes were considered. The first is the addition of a control valve in the pump delivery chamber, as shown in Fig. 11. This valve must open and release any excess elastic energy at the correct time and with the correct rates in order to damp the transient pressures and eliminate after-injection. The second alternative is to redesign the pump spill port and pump delivery valve to insure that the excess elastic energy is released at the pump during the spill period.

AVERAGE ELASTIC ENERGY RELEASE VIA ADDITIONAL CONTROL VALVE

The control valve concept introduced in this paper is similar to the duplex or two-way delivery valves which have been experimentally investigated. This paper contributes a calculation procedure which can be used by the design

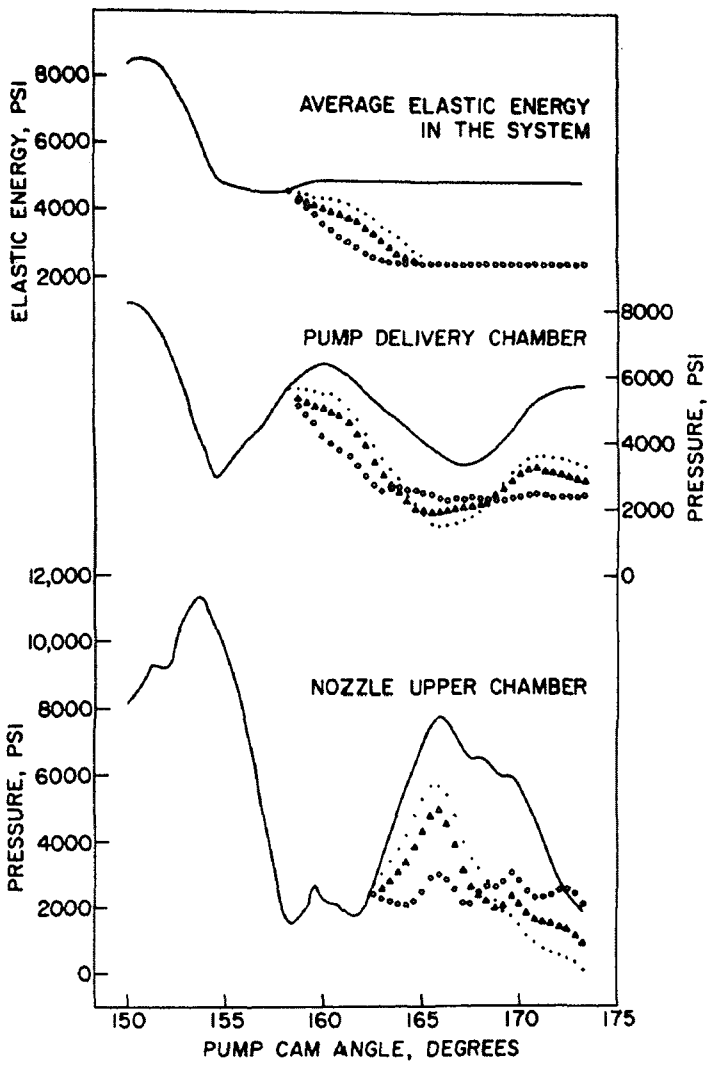

Fig. 13 - Injection system variables versus pump cam angle. Effect of the shape of the average elastic energy drop. Control valve approach, test 4 (Table 1)

engineer to determine when and how this valve should be operated.

An arbitrary release of fuel through a valve during the desired control period is likely to be unsuccessful as far as satisfying the objectives. The following few alternatives point out some of the complications. Figs. 12 and 13 illustrate the interaction of the time-variant average elastic energy and pressure transients in the system. All traces in these figures begin at the beginning of the control period. The solid traces represent the system performance without alterations. The appearance of high residual energy in the solid traces and the existence of negative pressures in some of the traces are due to the fact that after-injection and cavitation were not accounted for in the design program.

Two alterations are given in Fig. 12 to illustrate the dependence of pressure on the time of initiating the elastic energy drop. The results given in this figure represent test 1 (Table 1 and Fig. 2). The circles represent an elastic energy drop starting at the point of delivery valve closing while the triangles represent an energy drop starting at the point of needle final closing. From comparisons of resulting pressures at the nozzle upper chamber, the following is clear: The first alteration (given by circles) results in added cavitation. Also, after-injection is liable to occur since the residual pressures at the injector are not damped. The second alteration (given by triangles) results in damping the residual pressures and therefore after-injection will not occur. Also, no cavitation is detected in the second example. Thus it can be concluded that an elastic energy drop beginning at the point of final needle closing is desirable. Several other trials have confirmed this conclusion.

Several shapes of elastic energy drop were studied and three of them are given in Fig. 13. Results in this figure are for test 4 (Table 1 and Fig. 5). In this figure, all alterations

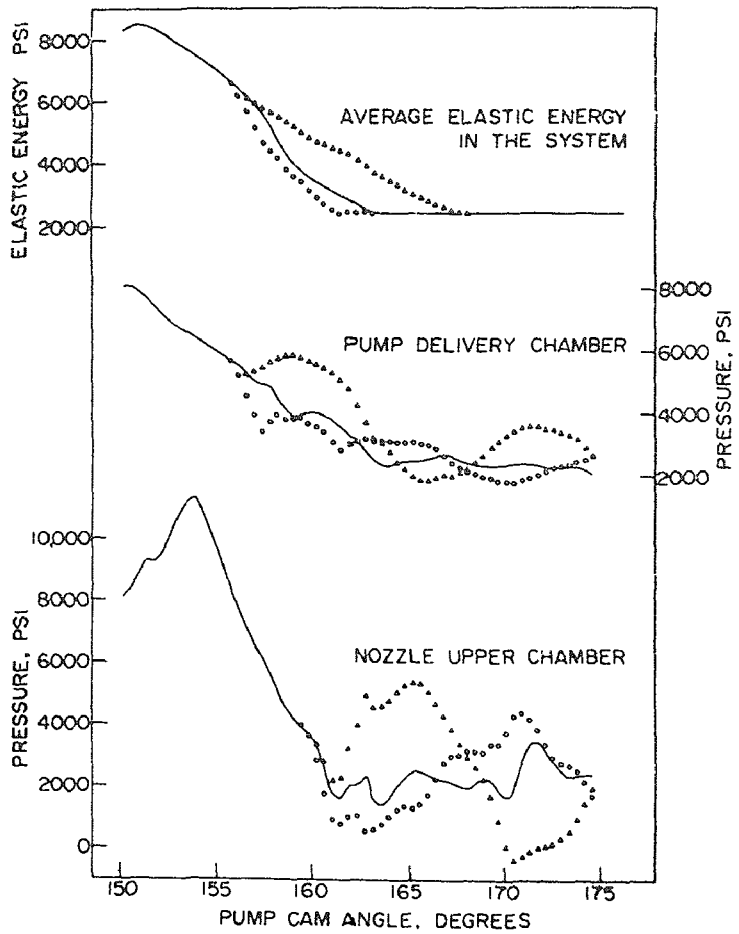

Fig. 14 - Injection system variables versus pump cam angle. Effect of the rate of the average elastic energy drop. Redesigned spill port approach, test 4 (Table 1)

begin at the point of final needle closing. The three elastic energy alterations are represented by dots, triangles, and circles. By comparing pressures at the nozzle upper chamber, it is clear that the average elastic energy function represented by the circles results in damping the residual pressures and thus eliminates after-injection. The other two alterations reduce the magnitude of the resulting pressures but do not completely eliminate the possibility of after-injection.

AVERAGE ELASTIC ENERGY RELEASE VIA THE PUMP SPILL PORT

The second approach deals with redesigning the pump spill port. The object of the new design is to release the high elastic energy in the system by controlling the flow of fuel from the spill port. To allow this, the pump delivery valve must be open during a relatively long control period. This can be done by using slower rates of energy release and by employing delivery valves with high unloading volumes.

Several choices of average elastic energy functions are given in Figs. 14 and 15. Results in both figures are for test 4 (Table 1 and Fig. 5). Traces on these figures are used to illustrate the effect of the average elastic energy on the transient pressures in the system. Three of these functions are given in Fig. 14 and are used to illustrate the effect of changing the rate of elastic energy drop near the end of the control period on the resulting transient pressures. It is seen from this figure that the solid trace represents a desirable solution; the cases represented by circles and triangles are undesirable. The triangles represent a very slow drop of the elastic energy function. The very slow drop results in high residual pressures at the nozzle upper chamber which will prolong the main injection period. The circles represent a relatively fast elastic energy drop. This change results in high nozzle upper chamber pressures which lead to after-injection. The solid trace of the elastic energy function results in damping the residual pressures and eliminating the possibility of after-injection.

Fig. 15 is intended to illustrate the effect of the manner of variation of average elastic energy on the resulting transient pressure. Three functions are given to demonstrate this effect. All three functions in this figure have the same beginning and end points for the average elastic energy function. The solid average elastic energy trace represents a desirable solution since it results in damping the nozzle upper chamber

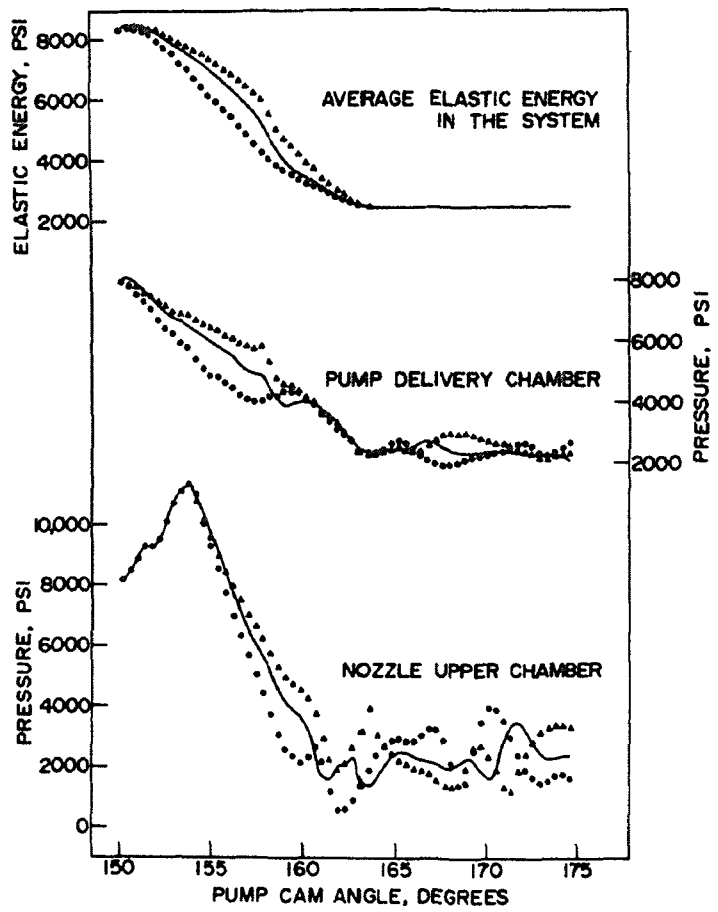

Fig. 15 - Injection system variables versus pump cam angle. Effect of the shape of the average elastic energy drop. Redesigned spill port approach, test 4 (Table 1)

pressures, therefore eliminating after-injection. The other two traces (triangles and circles) have less damping effect on the transient pressures than the solid line trace. Also, the trace given by triangles will result in prolonged injection period due to the relatively high pressures near the end of injection.

Usually no more than four trials were needed to achieve a desirable average elastic energy trace for both designs. It should be noted that the procedures described here for the formulation and application of the design program are general and could be used with any injection system. However, the results presented here apply only for the specific injection system described in this study.

CONCLUSIONS

The computer simulation used in this study accurately imitates the physical system behavior and therefore may be used confidently to study the diesel injection system. A critical evaluation of the various phenomena which influence performance is possible by parametric studies.

Injection system average elastic energy is shown to be a suitable and convenient parameter to be utilized for studies of design improvements. Unlike the very erratic time-variant pressure and flow variations in the system, the average elastic energy is a smooth function of time. Design variations to eliminate after-injection are realizable, and a theoretical procedure is presented to accomplish this objective. The implications of two possible design alterations are discussed. Futher amplification of the use of control devices and both theoretical and physical demonstrations of their ability to accomplish the defined objectives appear in the companion paper.

The design procedure described herein may be applied to other types of injection systems and to the solution of other injection problems. Additionally, the methods have application to other interactive fluid and mechanical systems which are characterized by undesirable high-frequency oscillations.

NOMENCLATURE

A	= pipe cross-sectional area or area of opening at orifice
a	= wave propagation velocity
C_d	= discharge coefficient

C_t	=	product of the nozzle injection holes area and the coefficient of discharge
D	=	pipe diameter
d	=	as a subscript, refers to pump delivery chamber
f	=	friction coefficient at valve or needle
f	=	Darcy-Weisbach friction factor
f	=	as a subscript, refers to pump feed chamber
g	=	acceleration of gravity
h	=	as a subscript, refers to nozzle injection holes
i	=	as a subscript, refers to injection chamber
INJ	=	as a subscript, refers to equivalent pipe length of injector volume
K	=	bulk modulus of elasticity
k	=	spring force
l	=	as a subscript, refers to nozzle lower chamber
n	=	as a subscript, refers to injector needle
p	=	pressure
p	=	as a subscript, refers to pumping chamber
PUMP	=	as a subscript, refers to equivalent pipe length of the pump delivery chamber volume
Q	=	volumetric flow rate
r	=	spring stiffness
S	=	valve or needle displacement
t	=	time
TOT	=	as a subscript, refers to total pipe length including equivalent lengths of volume at pump and injector
u	=	as a subscript, refers to upper nozzle and delivery chamber
V	=	velocity
V	=	volume of fluid enclosures in pump and injector
v	=	as a subscript, refers to delivery valve
W, X, Y, Z	=	as subscripts, refer to positions in the x-t plane
w	=	weight of valve or needle
x	=	distance
Zd	=	as a subscript, is the instantaneous flow in the delivery pipe at the pump delivery chamber
Zs	=	as a subscript, is the instantaneous flow in the supply pipe at the pump feed chamber
Zu	=	as a subscript, is the instantaneous flow in the delivery pipe at the injector
γ	=	specific weight of fluid

ACKNOWLEDGMENT

The financial support of the Environmental Protection Agency through research grant No. R800424 is gratefully acknowledged. This work was also assisted by research funds provided by the Chevron Research Co. The valuable assistance of S. Onyegegbu, PhD student at the University of Michigan, is also appreciated.

REFERENCES

1. C. H. Bradbury, "Stationary Compression Engines." London: E. & F. N. Spon. Ltd., 1950.
2. A. C. Rosselli, Manager of Controls and Fuel Systems, Cummins Engine Co., personal communication, July 13, 1972.
3. Jay A. Bolt and M. F. El-Erian, "Diesel Ignition, Combustion and Emissions." Progress Report No. 19 submitted to the U.S. Army-Tank Automotive Command, Warren, Michigan, September 1972.
4. W. P. Mansfield, "A New Servo-Operated Fuel Injection System for Diesel Engines." SAE Transactions, Vol. 74 (1966), paper 650432.
5. A. Dolenc and R. Lees, "Some Aspects of the Development of the OVA24 Traction Engine." Proc. Inst. Mech. Engrs., Vol. 183, Part 3b, 1968-1969, p. 24.
6. G. Lustgarten and A. Dolenc, "Development of Injection System for Medium-Speed Diesel Engine with Quiescent-Type Combustion Chamber." Diesel Combustion Symposium, Inst. Mech. Engrs., London, April 1970.
7. G. A. Becchi, "Analytical Simulation of Fuel Injection in Diesel Engines." SAE Transactions, Vol. 80 (1971), paper 710568.
8. B. E. Knight (M.A.), "Fuel Injection System Calculations." Proc. Inst. Mech. Engrs. (A.D.), No. 1, 1960-1961.
9. E. B. Wylie, J. A. Bolt, and M. F. El-Erian, "Diesel Fuel Injection System Simulation and Experimental Correlation." SAE Transactions, Vol. 80 (1971), paper 710569.
10. V. L. Streeter and E. B. Wylie, "Hydraulic Transients." New York: McGraw-Hill Book Co., 1967.
11. M. F. El-Erian, "Simulation and Control of Transient Flow in the Diesel Injection System." PhD thesis, University of Michigan, April 1972.

APPENDIX
THE INJECTION SYSTEM EQUATIONS

The equations describing the injection system are divided into three categories: pump equations, injector equations, and pipe equations. These equations are summarized below. Further information concerning these equations and their solutions can be found in Refs. 9 and 11.

PUMP EQUATIONS

The pump equations written for the feed chamber, pumping chamber, and delivery chambers (shown in Fig. A-1) are given below, respectively.

$$\frac{dp_f}{dt} = \frac{K_f}{\forall_f}(Q_{Zs} - Q_1 + Q_2 - Q_4) \qquad \text{(A-1)}$$

$$\frac{dp_p}{dt} = \frac{K_p}{\forall_p + A_vS_v - A_pS_p}(A_pV_p - A_vV_v + Q_1 - Q_2 - Q_3) \qquad \text{(A-2)}$$

$$\frac{dp_d}{dt} = \frac{K_d}{\forall_d - A_vS_v}(A_vV_v + Q_3 - Q_{Zd}) \qquad \text{(A-3)}$$

Each of the above equations is a combination of continuity and compressibility equations written for a particular volume. In addition, the delivery valve equations are given by:

$$\frac{dV_v}{dt} = \frac{g}{w_v}(A_v(p_p - p_d) - k_v - r_vS_v - f_vV_v) \qquad \text{(A-4)}$$

$$\frac{dS_v}{dt} = V_v \qquad \text{(A-5)}$$

INJECTOR EQUATIONS

These equations take a similar form and are written for the injection delivery and nozzle upper chamber, the nozzle power chamber, and the injection chamber (Fig. A-2), respectively:

$$\frac{dp_u}{dt} = \frac{K_u}{\forall_u + A_uS_n}(Q_{Zu} - Q_5 - Q_8 - A_uV_n) \qquad \text{(A-6)}$$

$$\frac{dp_l}{dt} = \frac{K_l}{\forall_l + A_lS_n}(Q_5 - Q_6 - A_lV_n) \qquad \text{(A-7)}$$

$$\frac{dp_i}{dt} = \frac{K_i}{\forall_i + A_iS_n}(Q_6 - Q_7 - A_iV_n) \qquad \text{(A-8)}$$

Additionally, the needle motion is described by the following two equations:

$$\frac{dV_n}{dt} = \frac{g}{w_n}(A_up_u + A_lp_l + A_ip_i - k_n - r_nS_n - f_nV_n) \qquad \text{(A-9)}$$

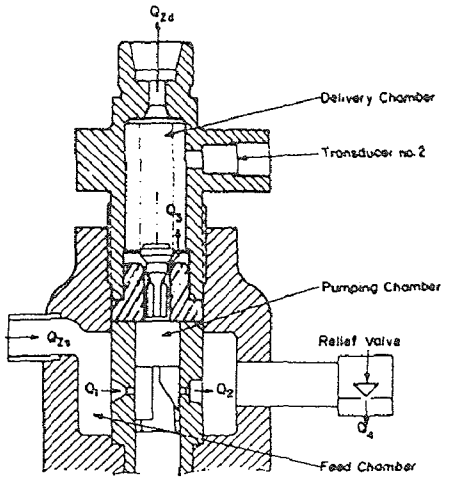

Fig. A-1 - Sectional view of injection pump

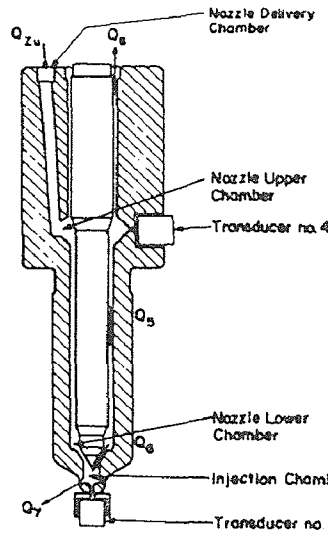

Fig. A-2 - Sectional view of injection nozzle

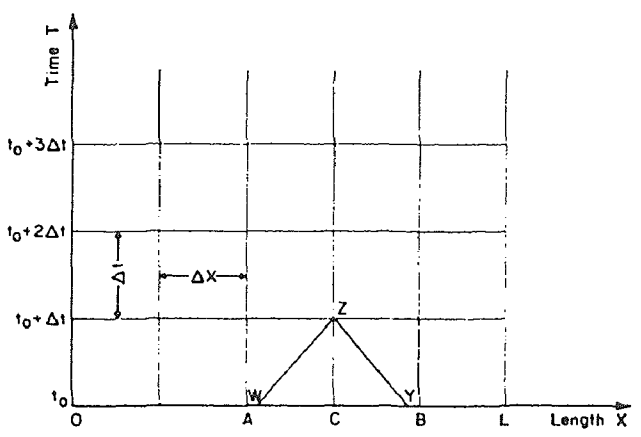

Fig. A-3 - Characteristics in x-t plane

$$\frac{dS_n}{dt} = V_n \qquad \text{(A-10)}$$

PIPE CHARACTERISTIC EQUATIONS

The equations are written in finite difference form for a pipe section of length X and a time period t (Fig. A-3) as follows:

$$Q_Z - Q_W + \frac{gA}{\gamma_W a_W}(p_Z - p_W) + \frac{f_W \Delta t Q_W |Q_W|}{2\,DA} = 0 \qquad \text{(A-11)}$$

$$x_Z - x_W = a_W \Delta t \qquad \text{(A-12)}$$

$$Q_Z - Q_Y - \frac{gA}{\gamma_Y a_Y}(p_Z - p_Y) + \frac{f_Y \Delta t Q_Y |Q_Y|}{2\,DA} = 0 \qquad \text{(A-13)}$$

$$x_Z - x_Y = -a_Y \Delta t \qquad \text{(A-14)}$$

Eq. A-11 is called the C^+ characteristic and is valid only along a line WZ described by Eq. A-12 and shown in Fig. A-3. Eq. A-13 is called the C^- characteristic and is valid only along a line WY described by Eq. A-14. With known initial conditions at points Y and Z (Fig. A-3), pressure and flow conditons at point W can be found by solving Eqs. A-11 and A-13.

This paper is subject to revision. Statements and opinions advanced in papers or discussion are the author's and are his responsibility, not the Society's; however, the paper has been edited by SAE for uniform styling and format. Discussion will be printed with the paper if it is published in SAE Transactions. For permission to publish this paper in full or in part, contact the SAE Publications Division.

Persons wishing to submit papers to be considered for presentation or publication through SAE should send the manuscript or a 300 word abstract of a proposed manuscript to: Secretary, Engineering Activities Board, SAE.

Society of Automotive Engineers, Inc.
TWO PENNSYLVANIA PLAZA, NEW YORK, N.Y. 10001

20 page booklet. Printed in U.S.A.

Fleet Week 73

FLEET OWNER

MOTOR & EQUIPMENT MANUFACTURERS ASSN

SOCIETY OF AUTOMOTIVE ENGINEERS, INC.
Two Pennsylvania Plaza, New York, N.Y. 10001

Analysis and Control of Transient Flow in the Diesel Injection System Part II – Design Results of Controlled After-Injection

Mohamed F. El-Erian, E. Benjamin Wylie, and Jay A. Bolt
University of Michigan

SOCIETY OF AUTOMOTIVE ENGINEERS

Combined Commercial Vehicle Engineering & Operations and Powerplant Meetings
Chicago, Ill.
June 18-22, 1973

730662

TABLE OF CONTENTS

Abstract . . . . . .
Calculation of Design Changes at the Pump . . . . . .
The Additional Control Valve Design . . . . . .
The Redesigned Pump Spill Port . . . . . .
Design Results and the Computer Simulation Confirmations of the Additional Control Valve Design . . . . . .
Design Results and the Computer Simulation Confirmations of the Redesigned Pump Spill Port . . . . . .
Experimental Verification of the Redesigned Pump Spill Port Approach . . . . . .
Experimental Modifications . . . . . .
Comparisons Between Experimental Results of the Original and Modified Systems . . . . . .
Conclusions . . . . . .
Nomenclature . . . . . .
Acknowledgment . . . . . .
References . . . . . .

Copyright ©Society of Automotive Engineers, Inc. 1973
All rights reserved.

730662

Analysis and Control of Transient Flow in the Diesel Injection System Part II – Design Results of Controlled After-Injection

Mohamed F. El-Erian, E. Benjamin Wylie, and Jay A. Bolt
University of Michigan

MANY DIESEL FUEL injection problems are related to the wave propagation phenomena in the pipeline connecting the pump and the injector. Most of these problems such as after-injection, cavitation, and needle impact may be controlled by controlling fuel release after the end of the main injection. However, due to the complexity of the fuel injection system, past control methods have largely depended upon cut-and-try experimental procedures and upon the use of many simplifying assumptions in analytical studies.

Several experimental procedures have been used to attack the problem of after-injection. Guglielmotti (1)* used different types of vented pump delivery valves to reduce the injection system residual pressure. However, the reduced residual pressures resulted in cycle-to-cycle irregularities of injection characteristics at low-speed and load conditions. Lustgarten and Dolenc (2) were able to assume quasi-static conditions for

*Numbers in parentheses designate References at end of paper.

ABSTRACT

After-injection is the introduction of additional fuel to the combustion chamber after the end of the main injection. It is a persistent diesel fuel injection problem which usually results in reduced engine power and economy and increased emissions. After-injection is caused by uncontrolled pressure transients at the injector after the opening of the pump spill port. These pressure transients are related to the wave propagation phenomena in the high-pressure pipeline connecting the pump and injector. Use of experimental trial-and-error methods in attempts to control this phenomenon has met with limited success.

The analytical control method described in another paper is used to determine design means by which after-injection may be controlled. Further investigation and evaluation of two design changes which release the injection system excess elastic energy in a controlled manner are considered herein. One design change is the addition of a control valve in the pump delivery chamber. The other is the modification of the pump spill port. In both cases, pressures and flows are not altered during the main injection period. The ability of both design changes to control after-injection is confirmed by use of a simulation program. Experimental data from a system with the pump spill port modified in accordance with theoretical design calculations provide satisfactory confirmation of the analyses.

their injection system which was characterized by short fuel lines and relatively small dead volumes. Their model neglected the effect of fluid elasticity and wave propagation in the high-pressure pipeline. Under these assumptions they were able to calculate a pump spill port area which resulted in reducing after-injection while maintaining desirable pipe residual pressures.

In part I of this paper (3), the injection system stored elastic energy was investigated as a useful design control parameter. A control technique was described in which improved injection characteristics were obtained by specifying the stored elastic energy in a controlled manner. In this second part, results of studies of two improved designs are presented. The first is the addition of a control valve in the pump delivery chamber. This valve opens at the correct instant and releases the excess elastic energy in a controlled manner. In the second design, after-injection is eliminated by redesigning the pump spill port and pump delivery valve to control the rate of fuel spill. In both designs the original system pressure and flow conditions are not altered during the main injection period.

A computer simulation program is used to confirm the control method results. Also, calculated design modifications of the spill port and pump delivery valve are used to modify an actual injection system. Experimental comparisons between the original and modified injection system pressure characteristics are given to verify the validity of the design technique predictions.

CALCULATION OF DESIGN CHANGES AT THE PUMP

The design procedure described in part I of this paper (3) utilized an assumed average elastic energy profile and known initial conditions to calculate pressure and flow conditions in the whole x-t plane given in Fig. 10 (part I). To make use of these calculated conditions, they must be translated into feasible design changes in the injection system.

Two design changes at the pump, aimed at the elimination of after-injection, were suggested. The first design is a controlled relief valve in the pump delivery chamber which opens to release the excessive elastic energy at the correct instant. The second is a redesign of the pump spill port area to release the elastic energy in a controlled manner. In both designs, the calculated pressure and flow data at the pump-pipe boundary (p_d, Q_{Zd}) during the control period can be used as added boundary conditions to the pump equations (Eqs. A-1-A-5, part I). The solution of these equations provides the information to accomplish the desired design alterations. The equation and solution methods used in both designs are considered below.

THE ADDITIONAL CONTROL VALVE DESIGN - The control valve used in the first design is illustrated in Fig. 11 (part I). In order to maintain the injection pressures during the main injection period, it is assumed that this valve will open to release the excess elastic energy after the pump delivery valve closure. Therefore, the equation representing the pump delivery chamber (Eq. A-3, part I) is modified to:

$$\frac{dp_d}{dt} = -\frac{K_d}{\forall_d}\left(Q_{c.v.} + Q_{Zd}\right) \qquad (1)$$

where:

- p = pressure
- Q = volumetric flow rate
- K = fluid bulk modulus of elasticity
- $\forall$ = volume
- t = independent variable of time
- d = as subscript, refers to the pump delivery chamber
- c.v. = the additional control valve
- Zd = boundary at the pump delivery chamber and the pipe intersection

The flow through the control valve ($Q_{c.v.}$) is given by:

$$Q_{c.v.} = Cd_{c.v.}\, A_{c.v.} \sqrt{\frac{2g}{\gamma} p_d} \qquad (2)$$

where:

- Cd = coefficient of discharge
- A = area
- g = acceleration of gravity
- γ = weight of fluid per unit volume

The calculated pressures and flows (p_d and Q_{Zd}) at the pump-pipe boundary during the control period are used in Eqs. 1 and 2 together with a reasonable value of the valve coefficient of discharge of 0.7 to give the needed time-variable area of flow through the valve. Results of the computed area variations are discussed later.

THE REDESIGNED PUMP SPILL PORT - The second design determines a pump spill port area from the known pump-pipe boundary conditions (p_d, Q_{Zd}). This is done by solving the pump delivery chamber equation (Eq. A-3, part I) together with the delivery valve motion equations (Eqs. A-4 and A-5, part I). Each of these equations may be written in the following form:

$$\frac{dP}{dt} = \phi(t) \qquad (3)$$

where P is the dependent variable on the left side of the above equations and $\phi(t)$ is a function of time representing the right-hand side of these equations. Eq. 3 may be written in the following finite difference form:

$$\frac{P_2 - P_1}{\Delta t} = \phi(t_2) \qquad (4)$$

where the subscripts 1 and 2 refer to the beginning and end of the time period Δt. The left-hand side is the rate of change of the dependent variable with respect to time, and the time function on the right-hand side is calculated at the end of the

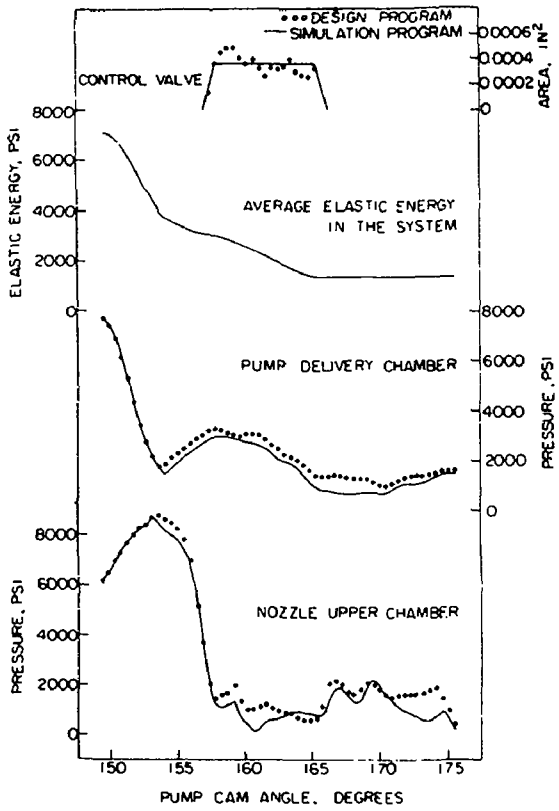

Fig. 1 - Design program results of injection system variables and simulation confirmation of these results. The additional control valve for test 1 (Table 1, part I)

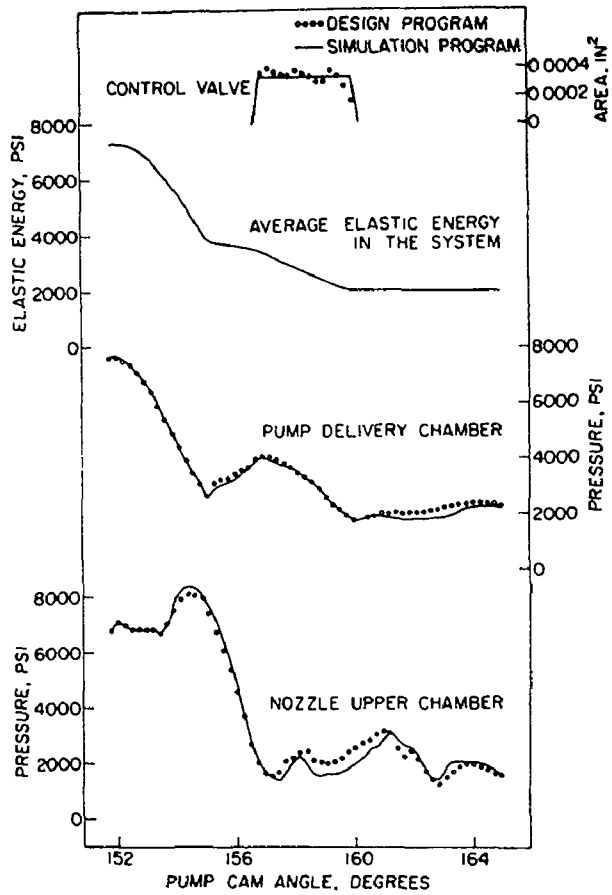

Fig. 2 - Design program results of injection system variables and simulation confirmation of these results. The additional control valve for test 3 (Table 1, part I)

period. It was found that the use of average values for the right-hand side during the period resulted in divergence of the solution due to the highly varying nature of the delivery valve velocity during the closing period. Extreme variations in the delivery valve velocity during the closing period result from the use of a light valve spring and the fact that the acting pressure force (p_d-p_p) is small and is highly varying. Converging solutions were obtained by using the finite difference form given by Eq. 4.

In the finite difference forms of Eqs. A-3-A-5 (part I), p_d and Q_{Zd} are known from previous calculations, and p_p, s_v, and V_v are the unknowns to be determined. These equations are solved by using an iterative procedure and a convergence technique described in Ref. 4.

The calculated pressure in the pump chamber (p_p) together with the calculated valve motion (s_v, V_v) are used in the finite difference form (Eq. 4) of the pumping chamber equation (Eq. A-2, part I) to determine the spill port area. For this equation, the feed chamber pressure (p_f) is assumed at a value of 150 psi on the basis of previous simulation results. It should be noted that the spill port area is highly insensitive to the value of p_f because p_f is much less than the pumping chamber pressure (p_p) during the major part of the spill.

DESIGN RESULTS AND THE COMPUTER SIMULATION CONFIRMATIONS OF THE ADDITIONAL CONTROL VALVE DESIGN

A study of the effect of timing and shape of the average elastic energy function on the system residual pressures was presented in part I. In this study, the average elastic energy curve given by circles in Fig. 13 (part I) represented a desirable solution for the after-injection problem. A control valve appended to the pump delivery chamber to release the system elastic energy in the controlled manner is one way to achieve the desired result. The area of flow through the control valve is calculated by the design program in the manner described by Eq. 2.

Design program results and simulation program confirmations of these results for tests 1, 3, and 4 (Table 1, part I) are given in Figs. 1, 2, and 3, respectively. In these figures the circles represent results obtained by the design program, while simulation program confirmations of these results are illustrated by solid traces. The traces include the system average elastic energy, pressures in the pump delivery chamber and injector upper chamber, and the area of flow through the control valve. It should be noted that a simple valve motion

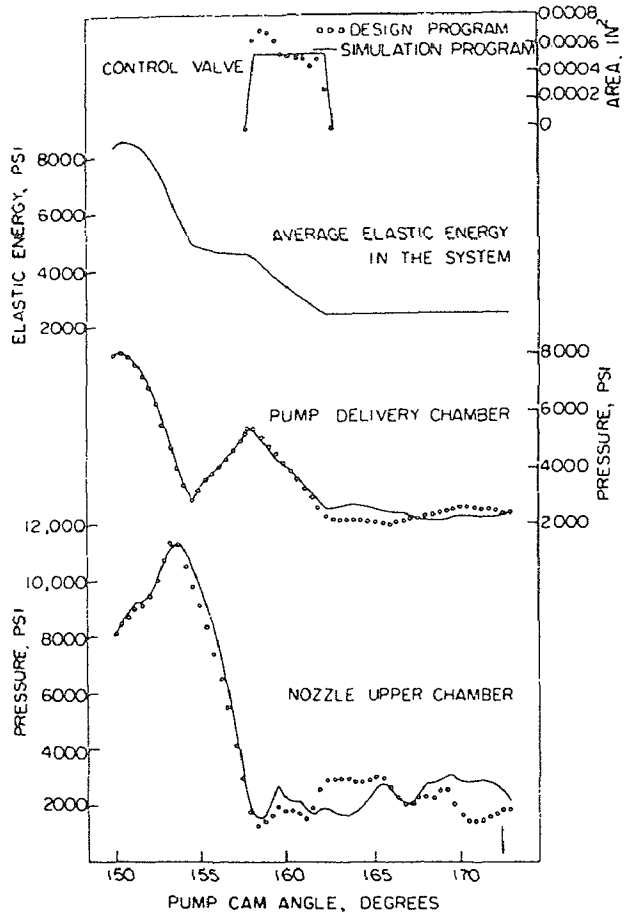

Fig. 3 - Design program results of injection system variables and simulation confirmation of these results. The additional control valve for test 4 (Table 1, part I)

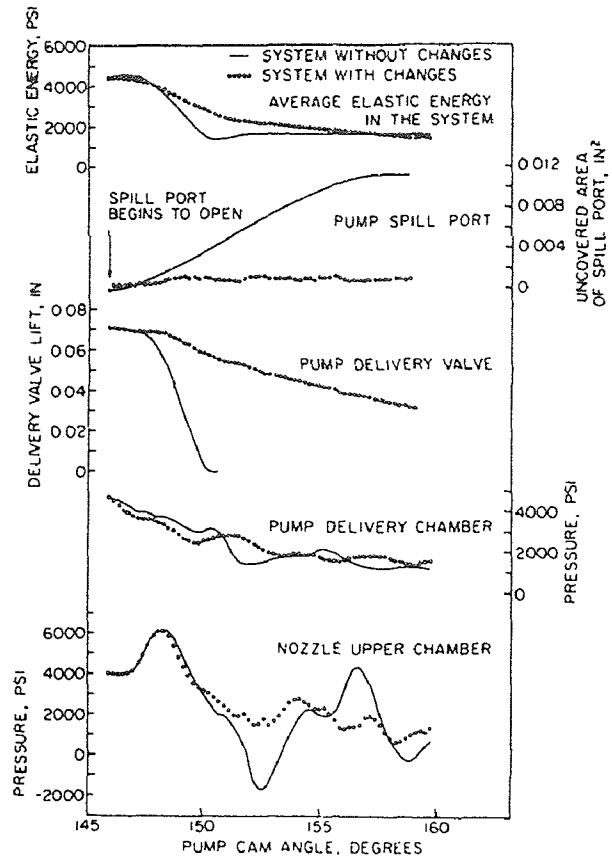

Fig. 4 - Comparisons of original injection system performance and design program results of the modified system. The redesigned spill port for test 2 (Table 1, part I)

was used in the simulation program. As a result, the valve area is described by a linear opening of the valve, a constant maximum opening area, and a linear closing. This area was obtained by averaging the design program results for the control valve areas, as shown in Figs. 1-3.

In all the cases presented, the control valve starts to open when the needle finally closes. The maximum opening area differs from one case to the other; the combined higher load and speed conditions require larger areas of flow through the control valve than the relatively lower speed and load conditions. The valve-opening periods for tests 3 and 4 (Figs. 2 and 3) are both 1.2 ms. However, these periods are different in terms of cam angle degrees due to the speed difference between the tests. The valve-opening period for test 1 (Fig. 1) is 2 ms. This is greater than for tests 3 and 4 primarily because of the relatively low base pressure associated with this test*.

The average elastic energy traces in Figs. 1-3 result in the damping of the system pressure oscillations and therefore the elimination of after-injection. It should be emphasized that the injection characteristics during the main injection period are not altered since the average elastic energy function during this period and the system base pressure are not changed. Simulation program results confirm the design program predictions. Small differences between design and simulation results can be attributed to use of the simpler valve motion in the simulation program.

DESIGN RESULTS AND THE COMPUTER SIMULATION CONFIRMATIONS OF THE REDESIGNED PUMP SPILL PORT

A study of the effect of the average elastic energy function for use with the redesigned pump spill port was presented in part I. In this study, the solid line average elastic energy trace in Figs. 14 and 15 represented a desirable solution to the after-injection problem. This solution is achieved by redesigning the pump spill port in order to release the system elastic energy in the desired controlled manner. Design results of the required spill port area together with the simulation program confirmations of these results are now presented for tests 2-4 (Table 1, part I).

The original system performance was illustrated in part I in Figs. 3-5. A comparison between this performance and the

*This test uses a different nozzle area than tests 3 and 4.

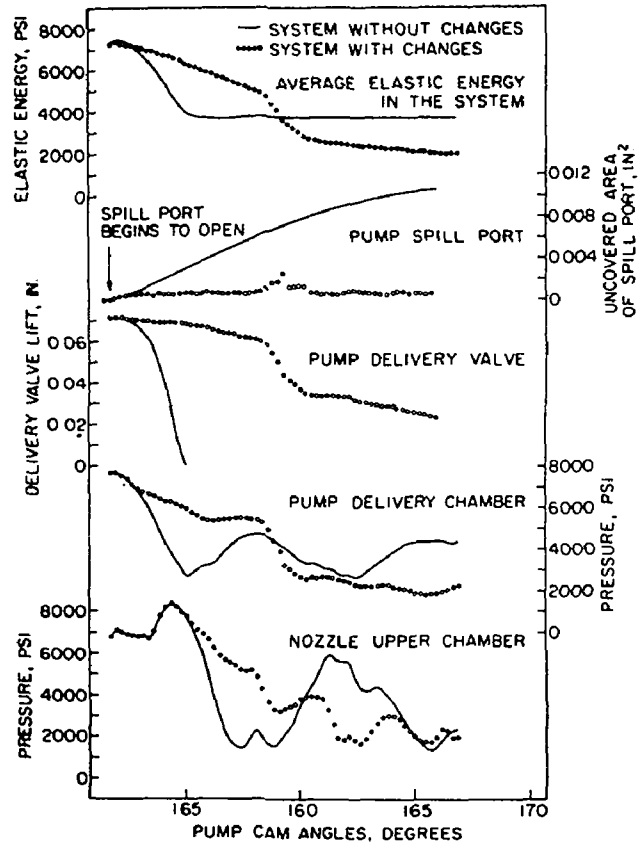

Fig. 5 - Comparisons of original injection system performance and design program results of the modified system. The redesigned spill port for test 3 (Table 1, part I)

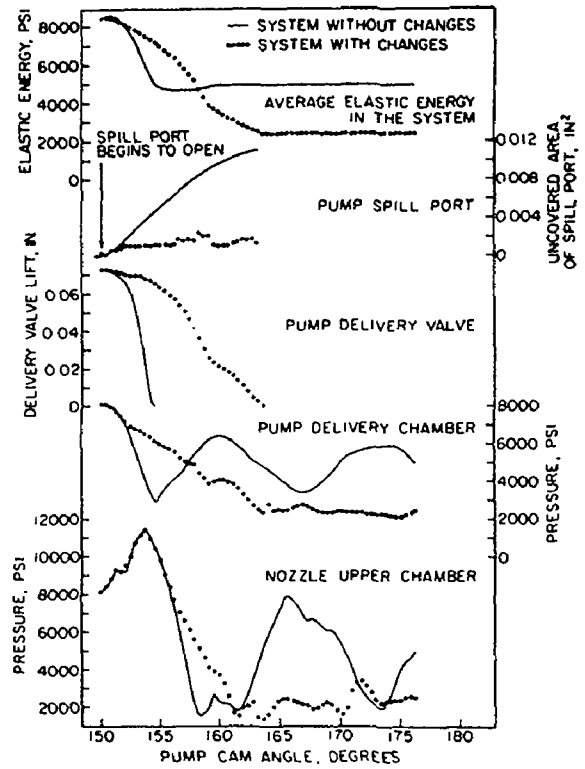

Fig. 6 - Comparisons of original injection system performance and design program results of the modified system. The redesigned spill port for test 4 (Table 1, part I)

modified system as calculated by the design procedure is given in Figs. 4-6 for tests 2-4, respectively. In these figures the solid traces represent the original system performance while the circles represent the modified one. Comparisons are given for the system average elastic energy, the pump spill port areas, the pump delivery valve motion, and for pressures in the pump delivery and nozzle upper chambers. As mentioned previously, the design procedure utilizes a controlled function for the average elastic energy to calculate the performance of the modified system. It may be observed in the figures that the design changes result in damping the pressure oscillations thereby eliminating after-injection. Most of the elastic energy release is accomplished at the pump by keeping the pump delivery valve open for longer periods compared with its original performance. This is achieved by use of the relatively smaller areas of the modified spill port and by use of a delivery valve that permits a higher unloading volume.

In all the cases, a delivery valve diameter of 0.374 in was used instead of the original diameter of 0.236 in. It should be noted that the resulting system base pressure for the modified system is the same as the original one, and that the resulting pressures at the injector for the modified system differ only slightly from the original system.

It may be noted in Figs. 4-6 that the resulting area of the pump spill port starts with a linear opening and then reaches a constant value. In Fig. 6, the spill port area begins to increase again near the end of delivery valve closing. The constant opening of the spill port is nearly the same in all cases (0.0011 in^2). Therefore, it is possible to describe a common spill port area as a function of pump plunger lift for all the reported cases. Such a common description is not possible in terms of time or pump cam angle because of the difference in speed for each test.

A common spill port area was used in the simulation program in order to confirm the design procedure results. The modified spill port areas are drawn as a function of pump cam angle and are compared with the original areas in Figs. 7-9. As mentioned previously, these modified areas would appear identical if they were drawn as functions of pump plunger lift. In the same set of figures, comparisons between the injection pressure characteristics for the modified and original systems indicate that slight differences occur for tests 2 and 3 while a relatively greater difference is observed with test 4. It should be noted that test 4 has high-speed and load conditions and high system base pressure (2400 psi). This relatively high base pressure is higher than the needle-closing pressure (2200 psi). Therefore, it can result in prolonging the injection period, as seen from Fig. 9. Better results for the system injection pressures were obtained by using a different area for the spill port, as seen in Fig. 10. The choice of this new area was directed toward lowering the system base pressure. This was achieved by using higher uncovering rates for the

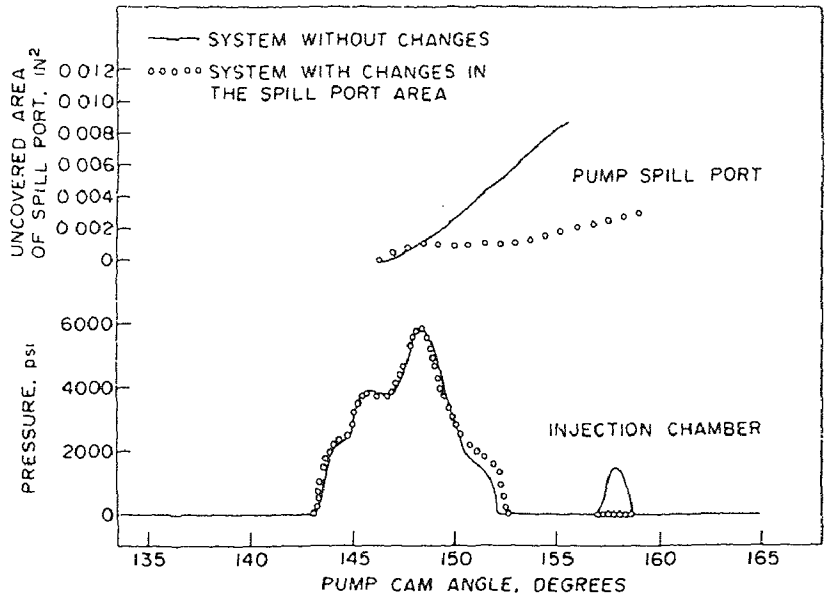

Fig. 7 - Comparison of injection chamber pressures of original and modified systems. The redesigned spill port for test 2 (Table 1, part I)

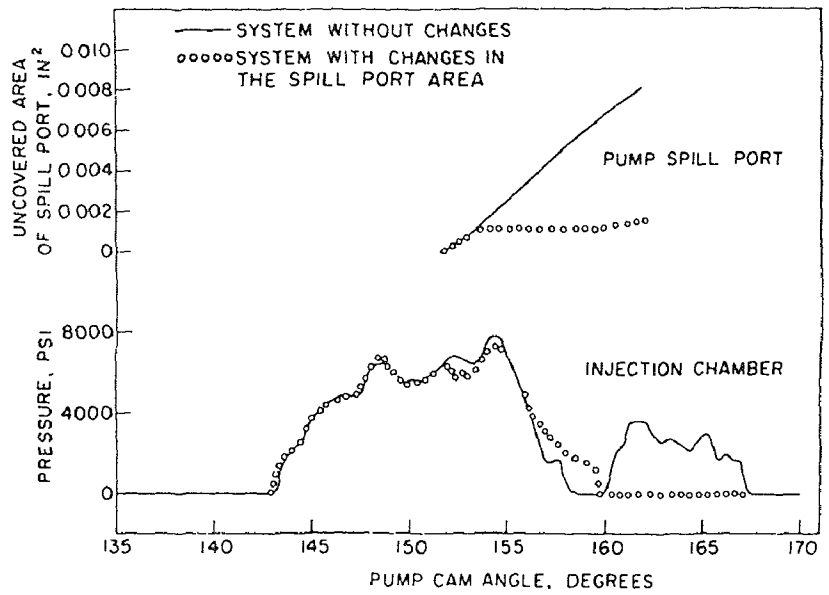

Fig. 8 - Comparison of injection chamber pressures of original and modified systems. The redesigned spill port for test 3 (Table 1, part I)

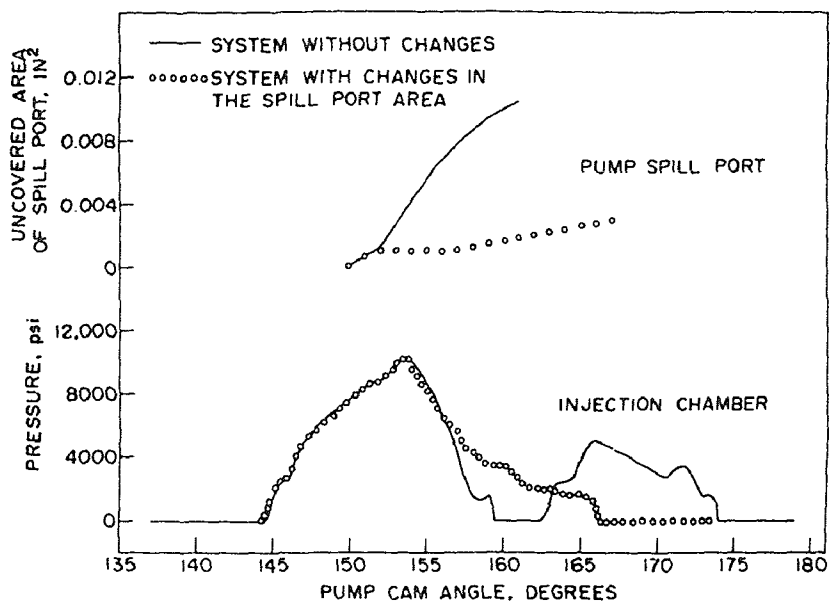

Fig. 9 - Comparison of injection chamber pressures of original and modified systems. The redesigned spill port for test 4 (Table 1, part I)

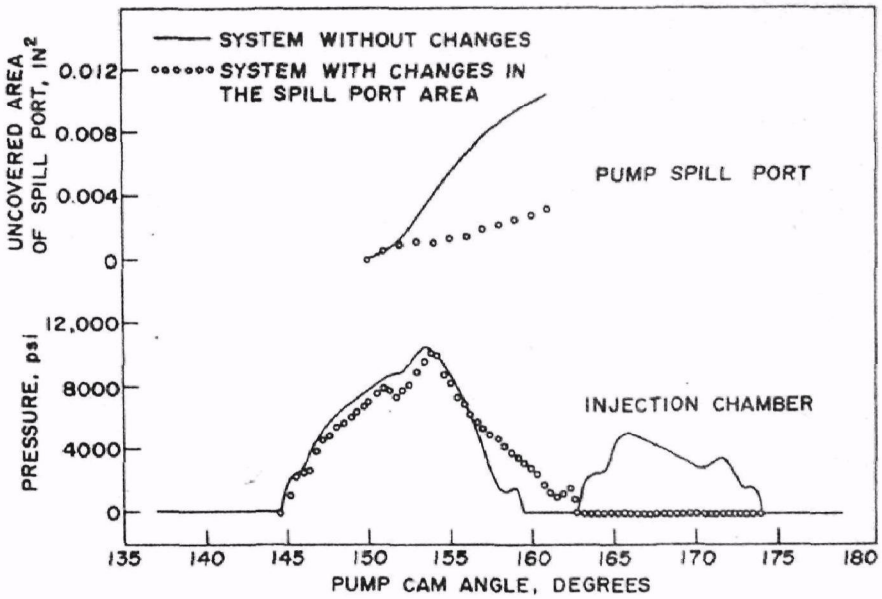

Fig. 10 - Comparison of injection chamber pressures of original and modified systems. The redesigned spill port for test 4 (Table 1, part I)

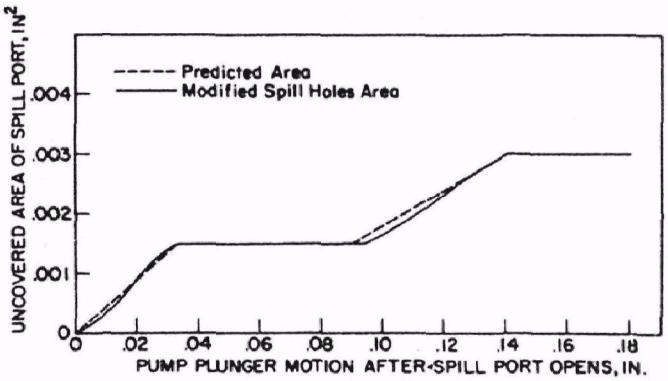

Fig. 11 - Comparison between the theoretically predicted spill area and the experimentally used one

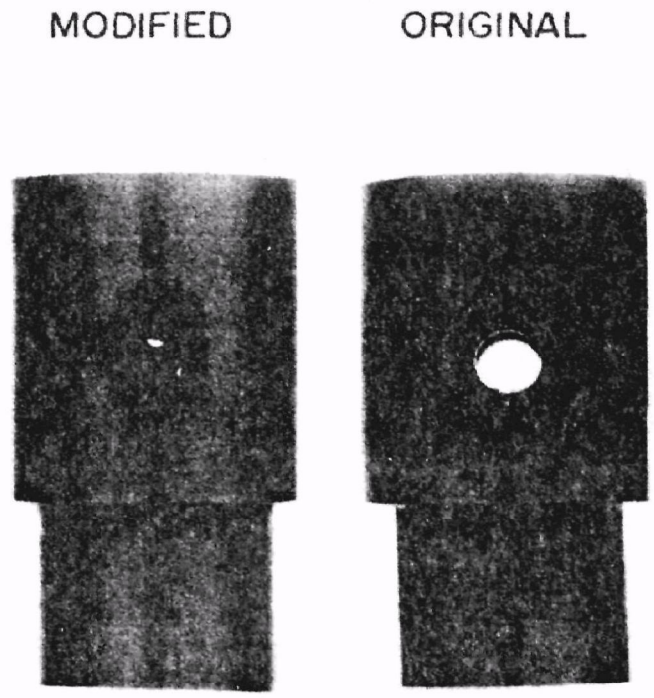

Fig. 12 - Comparison between original and modified spill ports

spill port near the end of injection while keeping these areas the same as those in Fig. 9 for the early part of the spill. The system base pressure for the results given in Fig. 10 was found to be 1600 psi.

The modified spill port area associated with test 4 and given in Fig. 10 was used in the simulation program to investigate its effect on tests 2 and 3. This area resulted in lowering the base pressures for these tests and also yielded a slight improvement in the injection pressure characteristics. However, extreme lowering of these base pressures at a combined low-load and speed condition (test 2) results in reaching vapor pressures. It should be noted that mechanical damage due to vapor bubble collapse is less harmful at combined low-speed and load conditions than at the combined high-speed and load conditions (2). Such minor conditions of temporary existence of vapor pressure may be tolerated if they only occur at low-load and speed conditions.

EXPERIMENTAL VERIFICATION OF THE REDESIGNED PUMP SPILL PORT APPROACH

The experimental system used in this study is a commercially available American Bosch injection system which consists of an APEIP type of pump and an ADB type of injection nozzle. This system is described in detail in Refs. 4 and

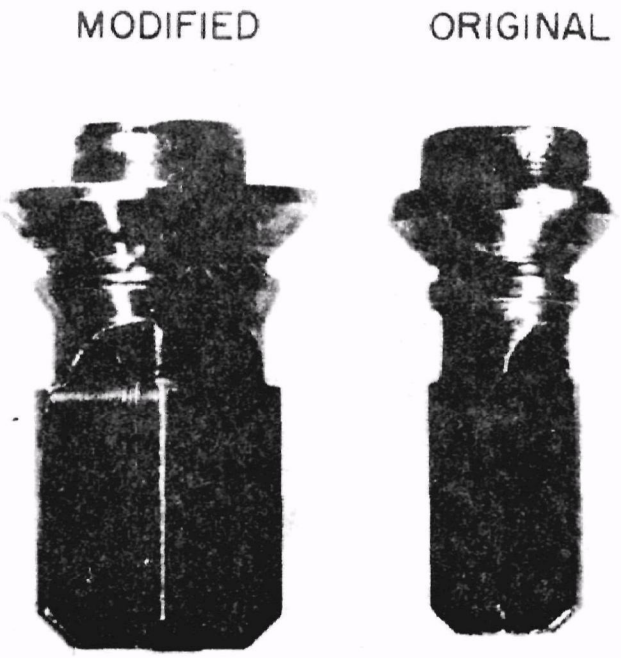

Fig. 13 - Comparison between original and modified pump delivery valves

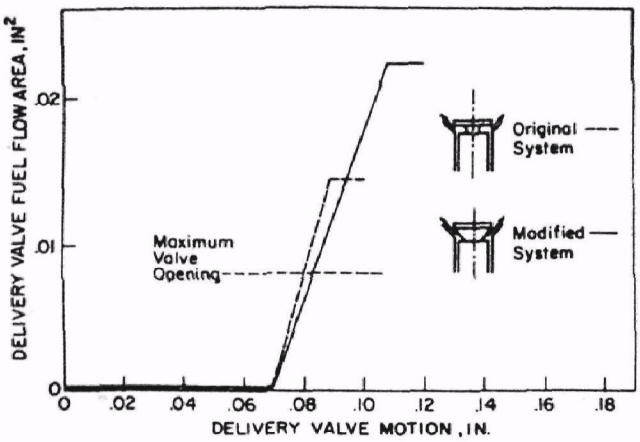

Fig. 14 - Fuel flow area past the delivery valve. Comparison of original and modified designs

5. It should be noted that this injection system is used by International Harvester Co. on the Army Tank Automotive Command research engine (the TACOM engine). This engine is used at the University of Michigan for combustion and emission research. Emission and performance studies on this engine (6) showed the adverse effect of after-injection and the need for eliminating it.

An experimental study was therefore carried out on the injection system to verify the validity of the theoretical results obtained from the application of the analytical control technique. Further combustion and emission studies of improved injection system characteristics are planned.

In the experimental study, after-injection was increased in the experimental system by using a restricted nozzle hole area. The original nozzle had four holes, 0.0128 in diameter each. The injection area was then reduced by passing a 0.010 in diameter steel wire through two of the injection holes. Under these conditions the product of the unrestricted injection area and the coefficient of discharge ($C_t = Cd \cdot A_h$) was found to be about 0.0002 in^2. Some variations in C_t of up to 10% were noticed and related to inaccuracies in the method used to reduce the injection area. The use of the above-reduced area resulted in the presence of after-injection over a large portion of the system-operating conditions. The control technique was used with the above conditions to predict the required design changes (spill port area and delivery valve diameter).

EXPERIMENTAL MODIFICATIONS - The predicted spill port area is shown in Fig. 11 as a function of the pump plunger motion. This area consists of a linear opening, followed by a constant area of 0.00151 in^2, and then another linear opening to reach a maximum opening of 0.00303 in^2. This was achieved by using a set of three circular holes. The modified area is also given in Fig. 11. In addition, a comparison between the original and modified spill port designs is given in Fig. 12. In the modified system, the lower two holes are each 0.31 in diameter and are located at the same angle as the plunger helix. These holes are used to achieve the first area opening described in Fig. 11. After the lower two holes are completely uncovered, the spill area remains constant at 0.00151 in^2 until the plunger helix starts to uncover the upper port. The upper port is 0.44 in diameter and is used to achieve the second area opening given in Fig. 11. After all three ports are uncovered, the spill area remains constant at 0.00303 in^2. It is clear from Fig. 11 that the actual design modifications are very close to the theoretically desired conditions.

The pump delivery valve was also redesigned in order to insure the existence of an open valve during the control period. It was found that the fuel flow areas past the delivery valve could be kept the same as the original valve. However, a larger valve diameter was needed to delay the valve closing until the end of the control period. A comparison between the modified and original delivery valves is given in Fig. 13. The modified valve had a diameter of 0.374 in while the original valve was 0.236 in in diameter. However, the fuel flow area past the delivery valve was kept approximately the same as the original system (Fig. 14) despite the use of a larger diameter valve. This was achieved by using a taper of 30 deg after the end of the valve collar, as shown in Fig. 13. Several other modifications of the pump body, delivery valve seat, valve spring, and pump delivery chamber were required to accommodate the new bigger valve. It should be noted that these changes were designed in a way to maintain the same original delivery chamber volume.

COMPARISONS BETWEEN EXPERIMENTAL RESULTS OF THE ORIGINAL AND MODIFIED SYSTEMS - Experimental data of the modified system were collected over a

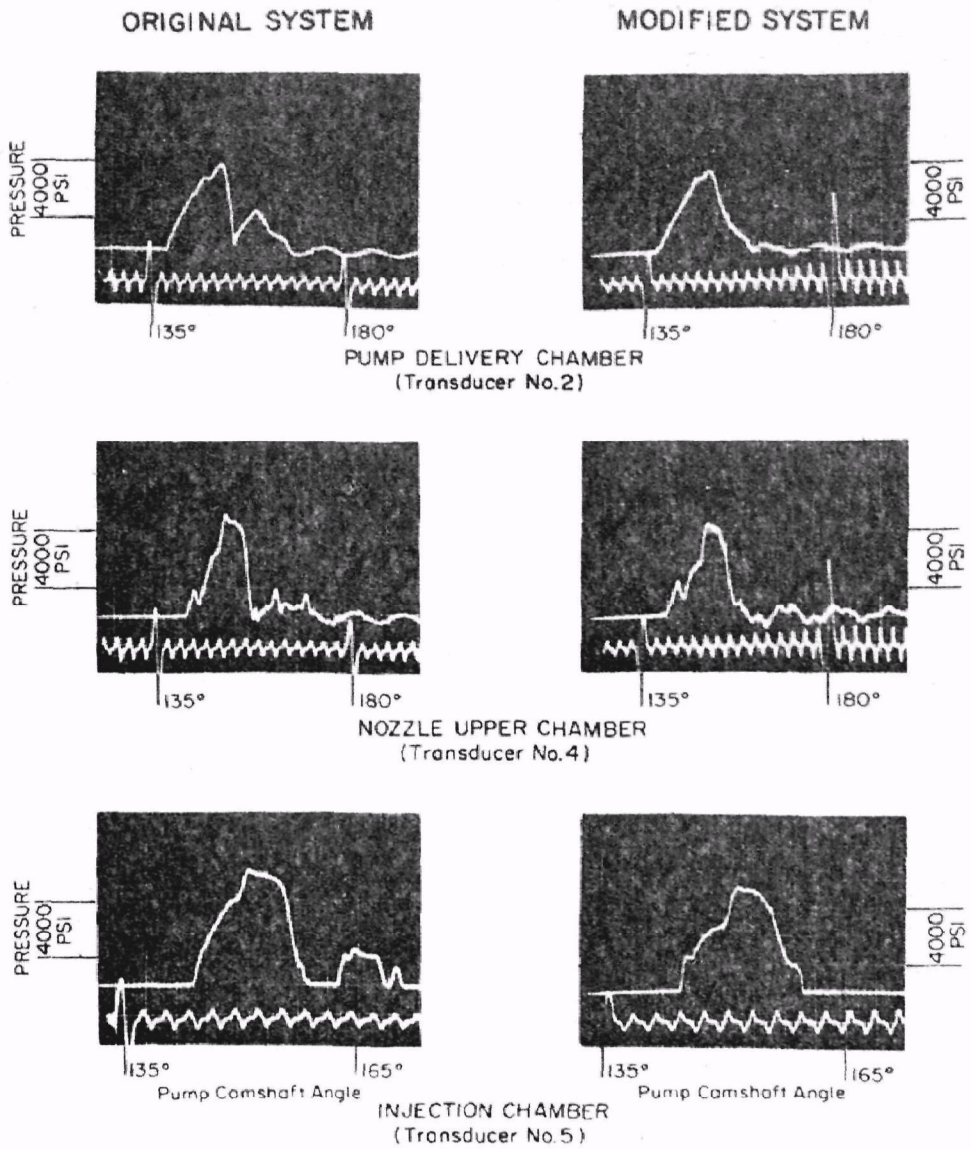

Fig. 15 - Comparison of injection system hydraulic characteristics, original and modified systems, 600 rpm pump speed and 60% of maximum fuel rack setting

wide range of speeds and fuel deliveries. These data were compared with the data previously collected with the original system. Samples of these comparisons are given in Figs. 15-17 for three cases of low, medium, and high after-injection of the original system. In each of the figures, comparisons are given between measured injection pressures at three different locations*: the pump delivery chamber, the nozzle upper chamber, and the nozzle injection chamber. All pressures in the above figures are given as a function of the pump cam angle.

*A schematic diagram of the injection system is given in Fig. 1, part I.

It is clear from the comparisons that the modified system transient pressures are controlled and damped after the end of the main injection while the original system pressures are relatively uncontrolled. After-injection was completely eliminated from the modified system performance in both Figs. 15 and 16, while a slight after-injection was present in Fig. 17.

Two important injection system characteristics may be noted from Figs. 15-17:

1. After-injection in the original system was caused by uncontrolled pressure transients at the pump delivery chamber. The pressure at the pump delivery chamber starts to drop sharply when the spill port opens. This pressure drop ends when the pump delivery valve is closed. At this point,

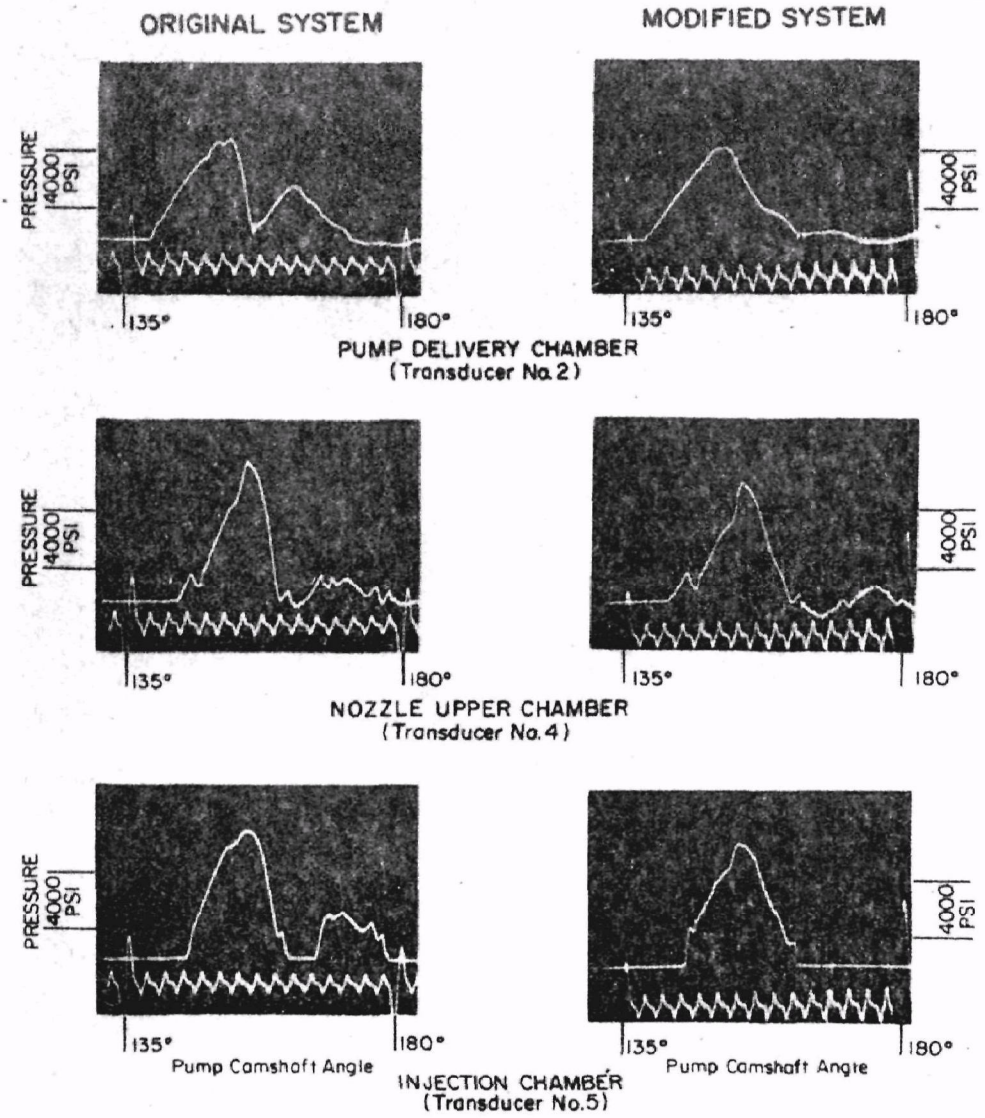

Fig. 16 - Comparison of injection system hydraulic characteristics, original and modified systems, 800 rpm pump speed and 60% of maximum fuel rack setting

the wave reflections result in a sharp increase of the pump delivery chamber pressure. This sharp increase is reflected in the pressures at the nozzle upper chamber and results in after-injection at the injection chamber.

2. The modified system pressures at the pump delivery chamber are decreasing at a slower rate than the original system; however, by the end of the spill period, the pump delivery chamber pressures are completely controlled. The slow drop at the pump delivery chamber is not reflected as a slow drop in either the nozzle upper or the injection chamber pressures.

It should be noted that it is widely accepted that a sharp pressure drop at the injector can only be achieved by a sharp pressure drop at the pump. Contrary to this belief, the results presented in Figs. 15-17 illustrate that a sharp pressure drop at the injector can be achieved while using a relatively slower rate of pressure drop at the pump.

The design objectives defined in part I of this paper were:

1. To control the transient pressures after the end of the main injection by damping them in a way to eliminate after-injection.

2. To maintain the pressure and flow characteristics during the main injection period.

Table 1 facilitates an assessment of the degree of success in achieving the above objectives. This is done by a comparison between important injection characteristics of both the original and modified injection systems at the three conditions presented in Figs. 15-17. In these comparisons, the maximum difference in base pressures was less than 18%, the maximum cycle pressure differed by less than 10%, the main injection

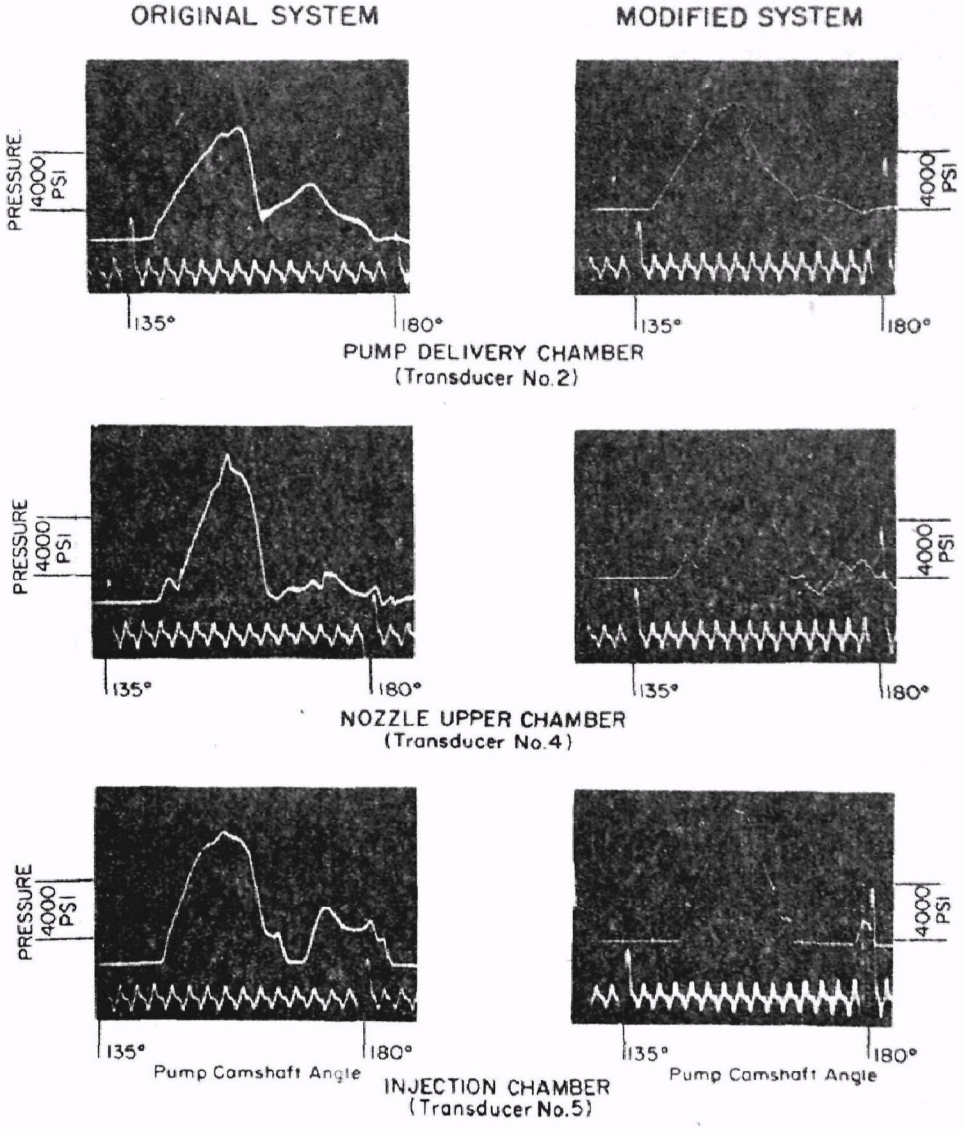

Fig. 17 - Comparison of injection system hydraulic characteristics, original and modified systems, 900 rpm pump speed and 70% of maximum fuel rack setting

Table 1 - Comparison Between Injection Characteristics of Both the Original and Modified Injection Systems at the Test Conditions Given in Figs. 15-17

Injection System	Original System			Modified System			Maximum Difference
Test Identification	I	II	III	I	II	III	is less than
Pump speed, rpm	600	800	900	600	800	900	–
Fuel rack setting as % of maximum rack travel	60	60	70	60	60	70	–
Base pressure, psia	2200	2000	2200	1800	2200	2400	18%
Maximum injection pressures, psia	8200	9100	9200	7400	8700	8600	10%
Main injection period, deg	14.94	17.02	21.8	15.45	18.60	21.2	10%
Fuel delivery during main injection, in^3/cycle	0.00868	0.00800	0.00947	0.00913	0.00895	0.01027	12%
Fuel delivery during after-injection, in^3/cycle	0.00282	0.00358	0.00491	0	0	0.00061	–

period differences were less than 10%, and the fuel delivery volume during main injection was within 12%. The above differences are due to many factors which include variations in the nozzle effective area and slight differences introduced by the design modifications, among others.

CONCLUSIONS

After-injection results from uncontrolled pressure transients after the end of the main injection period. Control of this undesirable phenomenon is possible by controlling the rates of pressure release at the pump. The injection system average elastic energy was shown to be a suitable and convenient control parameter which may be used to control undesirable injection pressure characteristics.

The control technique presented in this study allows a theoretical systematic design improvement of diesel injection characteristics. This was demonstrated by two improved designs in which the injection system pressures after the end of the main injection were controlled in order to eliminate after-injection. Such knowledge may be helpful in improving future injection systems and may lead to improved combustion and reduced exhaust emissions.

A redesigned pump spill port or a control valve appended to the pump delivery chamber may be used to eliminate after-injection. Either approach, if carefully designed, may be introduced without serious alterations in the injection system performance during the main period of injection. It was shown in this study that sharp pressure drops at the injector can be obtained while using slower rates of pressure drop at the pump.

Attempts to evaluate combustion characteristics of the newly developed system are being studied at the University of Michigan. Reduced emissions and increased efficiencies from using the modified injection system are anticipated benefits. A magnitude of injection pressures unattainable in the old system is also expected. Preliminary results indicate that after-injection from this system will be less sensitive to reductions in the injection holes area.

NOMENCLATURE

A = area of flow through the additional control valve
Cd = coefficient of discharge
C_t = time-averaged flow coefficient equal to the product of the nozzle holes area and its average coefficient of discharge
c.v. = as a subscript, refers to the additional control valve
d = as a subscript, refers to the pump delivery chamber
f = as a subscript, refers to the pump feed chamber
g = acceleration of gravity
h = as a subscript, refers to the nozzle injection holes
K = bulk modulus of elasticity
p = pressure
p = as a subscript, refers to the pumping chamber
P = used as a dummy variable in Eqs. 3 and 4
Q = volumetric flow rate
s = delivery valve lift
t = time
v = as a subscript, refers to the pump delivery valve
V = velocity of pump delivery valve
$\forall$ = volume
Zd = as a subscript, refers to the instantaneous flow in the delivery pipeline at the pump delivery chamber
γ = specific weight of fluid
Δt = time step
ϕ = a time function representing a time rate of change at the right-hand side of the pump equations

ACKNOWLEDGMENT

The financial support of the Environmental Protection Agency through research grant No. R800424 is gratefully acknowledged. This work was also assisted by research funds provided by the Chevron Research Co. The valuable assistance of S. Onyegegbu, PhD student at the University of Michigan, is also appreciated.

REFERENCES

1. A. Guglielmotti, "Influence of the Construction Characteristics of the Injection Pumps on Some Phenomena of Instability and Irregularity of Diesel Engine Operation." Tech. Bulletin, Vol. IX, No. 3 (July-September 1956), Fiat Co., Torino, Italy.
2. G. Lustgarten and A. Dolenc, "Development of Injection System for Medium-Speed Diesel Engine with Quiescent-Type Combustion Chamber." Diesel Combustion Symposium, Inst. Mech. Engrs., London, April 1970.
3. Mohamed F. El-Erian, E. Benjamin Wylie, and Jay A. Bolt, "Analysis and Control of Transient Flow in the Diesel Injection System, Part I—The Analytical Control Method." Paper 730661 presented at SAE Combined Commercial Vehicle Engineering and Operations and Powerplant Meetings, Chicago, June 1973.
4. M. F. El-Erian, "Simulation and Control of Transient Flow in the Diesel Injection System." PhD thesis, The University of Michigan, April 1972.
5. E. B. Wylie, J. A. Bolt, and M. F. El-Erian, "Diesel Fuel Injection System Simulation and Experimental Correlation." SAE Transactions, Vol. 80 (1971), paper 710569.
6. Jay A. Bolt and M. F. El-Erian, "Diesel Ignition, Combustion and Emissions." Progress report No. 19 submitted to the U.S. Army Tank Automotive Command, Warren, Michigan, September 1972.

This paper is subject to revision. Statements and opinions advanced in papers or discussion are the author's and are his responsibility, not the Society's; however, the paper has been edited by SAE for uniform styling and format. Discussion will be printed with the paper if it is published in SAE Transactions. For permission to publish this paper in full or in part, contact the SAE Publications Division.

Persons wishing to submit papers to be considered for presentation or publication through SAE should send the manuscript or a 300 word abstract of a proposed manuscript to: Secretary, Engineering Activities Board, SAE.

Society of Automotive Engineers, Inc.
TWO PENNSYLVANIA PLAZA, NEW YORK, N.Y. 10001

16 page booklet

Printed in U.S.A.

TECHNICAL REPORT DATA
(Please read Instructions on the reverse before completing)

1. REPORT NO. EPA-460/3-74-001	2.	3. RECIPIENT'S ACCESSION NO.
4. TITLE AND SUBTITLE Diesel Fuel Injection System Simulation and Experimental Correlation		5. REPORT DATE January, 1974
		6. PERFORMING ORGANIZATION CODE
7. AUTHOR(S) Jay A. Bolt		8. PERFORMING ORGANIZATION REPORT NO.
9. PERFORMING ORGANIZATION NAME AND ADDRESS University of Michigan, Department of Mechanical Engineering, Ann Arbor, Michigan 48104		10. PROGRAM ELEMENT NO.
		11. CONTRACT/GRANT NO. R800424
12. SPONSORING AGENCY NAME AND ADDRESS U.S. Environmental Protection Agency, Office of Air and Water Programs, Emission Control Technology Division, Ann Arbor, Michigan 48105		13. TYPE OF REPORT AND PERIOD COVERED 2/1/69 to 6/30/73
		14. SPONSORING AGENCY CODE
15. SUPPLEMENTARY NOTES		

16. ABSTRACT After-injection is the term used to describe the introduction of additional fuel into the combustion chamber of a diesel engine after the end of the normal injection. It is caused by uncontrolled pressure transients in the injection system. It is a persistent diesel fuel injection system problem which results in reduced engine power and economy and increased emissions.

A digital simulation of a conventional diesel fuel injection system was developed. The influence of such factors as wave propagation phenomena, pipe friction, and cavitation are included. The computer results are compared with transient pressures as measured on an actual fuel injection system operated on a test bench. The comparisons show the accuracy and validity of this simulation scheme. Analytical control methods were developed to help determine two design means by which after-injection may be controlled. These release the injection system excess elastic energy in a controlled manner. One design involves the modification of the pump spill port. Pressures and flow are not significantly altered during the main injection period. The ability of the system to control after-injection is confirmed by use of a simulation program and with experimental data.

17. KEY WORDS AND DOCUMENT ANALYSIS

a. DESCRIPTORS	b. IDENTIFIERS/OPEN ENDED TERMS	c. COSATI Field/Group
Diesel engines Fuel injection systems Hydraulic transients Exhaust emissions		

18. DISTRIBUTION STATEMENT Distribution is unlimited.	19. SECURITY CLASS (This Report) Unclassified	21. NO. OF PAGES 54
	20. SECURITY CLASS (This page) Unclassified	22. PRICE

EPA Form 2220-1 (9-73)

ENVIRONMENTAL PROTECTION AGENCY
Technical Publications Branch
Office of Administration
Research Triangle Park, N.C. 27711

OFFICIAL BUSINESS

AN EQUAL OPPORTUNITY EMPLOYER

POSTAGE AND FEES PAID
ENVIRONMENTAL PROTECTION AGENCY
EPA - 335

U.S. MAIL

Return this sheet if you do NOT wish to receive this material ☐, or if change of address is needed ☐. (Indicate change, including ZIP code.)